# Electron-photon interaction associated with uncertainty-based tunneling in a parallel double quantum dot

Kao-Chin Lin
*Physics Division, National Center for Theoretical Sciences, Hsinchu 30013, Taiwan*

Der-San Chuu
*Department of Electrophysics, National Chiao Tung University, Hsinchu, Taiwan*

(Received 20 July 2007; revised manuscript received 29 January 2008; published 20 March 2008)

The electron-photon interaction associated with the uncertainty based tunneling (EPAUT) in the parallel double quantum dot system is studied. In the considered system, the electron interacts with the single mode detuning quantum photon field, i.e., $\omega_{ph}+\Delta=\varepsilon_2-\varepsilon_1$, and transits between the quantum dots (QDs). The corresponding characteristic temperature is calculated and compared with the Kondo temperature to recognize the role of the related quantities. There are two energy uncertainties in the considered system. One is the energy difference between the energy of electron-photon interacting quasiparticle and the Fermi energy of the lead. The other is the detuning factor $\Delta$. Besides, $|\Delta/\pi|$ is the bandwidth of the intermediate state of EPAUT. The peak of the density of state corresponding to the EPAUT rises when the temperature is in the order of or below the characteristic temperature. The EPAUT peak can be modified via tuning the Fermi energy of the lead connected to the adjoined QD. Hence, the conductance between the connected leads is varied via tuning the Fermi energy of the lead connected to the adjoined QD.

DOI: 10.1103/PhysRevB.77.115339 PACS number(s): 72.15.Qm, 73.23.Hk, 73.40.Gk

## I. INTRODUCTION

Recently, due to the advancement of the fabrication technology of the semiconductor nanostructures, the electronic transport through nanostructure devices have been investigated extensively. One of the nanostructure devices is the quantum dot (QD) in which the electron energy levels are quantized and the behavior is similar to the atom. The QD is regarded as the artificial atom.[1] Similar to the atomic system, the coupled QD system can be treated as the artificial molecular system. The advantage of studying the QD systems is that the properties of artificial atom or molecular systems can be widely controlled by the external applied field. Hence, the QD systems have been used to implement the quantum optics, quantum device, e.g., the QD laser,[2,3] the single photon emitter,[4,5] and the cavity QED.[6–9] (for a review, see Ref 10). Besides, the quantum dot is one of the candidate of quantum information devices.[11–14] In the semiconductor cavity QED system, the QD is embedded in the semiconductor microcavity system, and the electron strongly couples with the quantum photon field and interacts coherently. The electron transition via the strong electron-photon interaction is reversible and the Rabi oscillation exists. In the cavity QED system, the electronic energy is split due to the Rabi oscillation and is called the Rabi splitting which has been observed in many experiments.[7–9]

In contrast to the natural atom or molecular system, the QD system is more convenient to connect with the lead; hence, the electron transport is an important subject in the QD system. For the application of the quantum optics and quantum electronic QD device, the electronic transport in the photon interacting QD system, i.e., the photon assisted transport (PAT), attracts many investigations.[15–17] (for a review, see Ref. 18). The pattern of Rabi splitting also emerges from the PAT in the double quantum dot or two states quantum dot and reflects on the profile of the PAT current or conductance.[19–22]

The uncertainty principle is one of the basic principle in quantum mechanics and affects the electronic transport. The Kondo effect is one of the quantum phenomena which is related to the uncertainty based electronic transport and has been experimentally observed in the QD system.[23] It is interested to ask: Is there any other quantum effect based on the uncertainty principle which may occur in the quantum dot or nanostructure devices? In this paper, we will explore a new quantum effect which is originated from the energy uncertainty related to the electron-photon interaction.

In this paper, we study the electron-photon interaction associated with the uncertainty based tunneling (EPAUT) in a double quantum dot (DQD) system. In our system, the electron can transit between the dots via absorbing or emitting a detuning photon and undergoes the uncertainty based tunneling (UT) between the QD and lead. There are two kinds of energy uncertainties in the EPAUT. One is related to the uncertainty based tunneling effect which is a crucial process in the Kondo effect. The other one is related to the electron-photon interaction, i.e., the detuning factor $\Delta$. The main process in our system is the EPAUT. In order to clarify the identities of these two uncertainties, we will firstly describe "the detuning factor and Rabi oscillation" and "the uncertainty based tunneling in Kondo effect" in the following.

### A. Detuning factor and Rabi oscillation

The Rabi oscillation is one of the processes in this paper. It is resulted from the periodic transition between two states in the two-level system. If the electron occupies the higher energy resonant state with energy $\varepsilon_2$ and interacts with the single mode detuning quantum photon field, i.e., $\omega_{ph}+\Delta=\varepsilon_2-\varepsilon_1$, the electron will transit to an intermediate state (nonresonant state for the case of nonzero detuning factor) with the energy $\omega=\varepsilon_2-\omega_{ph}=\varepsilon_1+\Delta$ via emitting a photon and retains to the higher resonant state via absorbing a photon.

 

After many cycles of the transiting processes, the resonant energy is split into the electron-photon interacting quasiparticle energies $\varepsilon_2^{ph\pm}=\varepsilon_2-\Delta/2\pm\Omega_{R,n_{ph}}/2$, where $\Omega_{R,n_{ph}}\equiv\sqrt{\Delta^2+4M^2n_{ph}}$ is the Rabi frequency and $M$ is the electron-photon coupling coefficient.[24] Similar to the higher energy state, the lower energy is split into $\varepsilon_1^{ph\pm}=\varepsilon_1+\Delta/2\pm\Omega_{R,n_{ph}}/2$. The Rabi splitting has been observed in many semiconductor device systems.[7,8]

An energy uncertainty $\Delta$ exists in the electron-photon interacting system when the photon is detuning. The zero photon number case gives a clear insight for understanding the role of detuning factor $\Delta$. For the zero photon case, the Rabi frequency is $\Delta$ and the period of the electron transition is $T=|2\pi/\Delta|$, i.e., the effective lifetime of the intermediate state is in the same order of magnitude of $|2\pi/\Delta|$ or the effective bandwidth is $|\Delta/2\pi|$. In the considered system, the detuning factor $\Delta$ is expected as an energy uncertainty related to the electron interacting with the detuning quantum photon field.

### B. Uncertainty based tunneling in Kondo effect

The uncertainty based tunneling is a crucial process in the Kondo effect.[23] In the simplest Anderson model, there is a local magnetic spin impurity embedded in the Fermi sea. The local spin of impurity can be exchanged with the Fermi sea via tunneling and causes the Kondo effect. In Anderson impurity model, the resonant energy of the electron in the magnetic impurity (or QD) is below the Fermi energy of Fermi sea; thus, the electron in impurity (or QD) is trapped and cannot tunnel out of the impurity to Fermi sea in the classical situation. Since there is a strong Coulomb interaction between the opposite spin electrons, the electron with opposite spin cannot exist in the impurity (or QD) at the same time. The only way for impurity (or QD) to exchange the spin state with the surrounding Fermi sea is to remove the electron from the impurity (or QD) into the surrounding Fermi sea first and then the electron in the surrounding Fermi sea with the spin opposite to the impurity tunnels into the impurity. The energy for an electron to be taken from the localized impurity state to the unoccupied state at Fermi surface is large and thus is forbidden classically without putting energy into the system. However, the tunneling between the localized magnetic impurity (or QD) and Fermi sea is allowed to happen due to the quantum uncertainty principle in a very short time interval around $h/|\varepsilon^F-\varepsilon_0|$, where $\varepsilon_0$ is the electron energy and $\varepsilon^F$ is the Fermi energy of the surrounding Fermi sea. The tunneling process via the allowance of the uncertainty principle is called UT in this paper. The electron in the localized impurity state tunnels into the electron reservoir via the UT, leaves the localized impurity state unoccupied, and becomes a virtual (intermediate) state with the effective bandwidth $D$.[25] Then, the electron in the Fermi sea with opposite spin tunnels into the impurity (or QD) and occupies the localized state. Eventually, the spin state of the impurity (or QD) is exchanged. When the temperature is in the same order of magnitude of or below a certain characteristic temperature, i.e., the Kondo temperature $T_K$, many of the spin exchange processes are taken place together, the Kondo effect occurs, and a peak is established around the Fermi energy of the electron reservoir, which is the famous "Kondo resonant peak." The Kondo temperature for the infinite onsite Coulomb interaction case is $T_K=D\exp[-\pi(\varepsilon^F-\varepsilon_0)/\Gamma]$.[26,27] The energy difference $(\varepsilon^F-\varepsilon_0)$ is the tunneling related energy uncertainty in the Kondo effect. $\Gamma$ is the coupling strength between the impurity (or QD) and lead.[25] Recently, the Kondo effect and the extension model have been studied intensively in the semiconductor quantum dot system.[23,28–32] Besides, no matter the original Anderson impurity model or the extension model, the Coulomb interaction is the necessary condition for the Kondo effect.

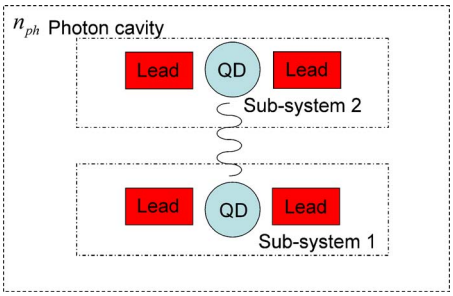


FIG. 1. (Color online) The sketch of the considered parallel double-quantum-dot system in the photon cavity. Each subsystem contains a QD coupled to two leads. The electron in QD can transit to the QD in the adjoined subsystem via electron-photon interaction.

Because of the requirement of the energy conservation, the electron cannot transit between the resonant states of the DQD via interacting with the detuning photon field. The energy uncertainty plays an important role that provides a way for the electron to transit between the nonresonant state and the resonant state. Hence, the electron can transit between the resonant states of QDs via the EPAUT. The EPAUT arises no matter the interdot Coulomb interaction exists or not; hence, the EPAUT is not equivalent to the "usual" Kondo effect. We will show that the Hamiltonian of the considered system can be transformed into the form of the Anderson impurity model. The electron photon interaction associated with tunneling is the necessary condition for the EPAUT. In the following, the characteristic temperature corresponding to the EPAUT is calculated and compared to the Kondo temperature to understand the roles of the uncertainties in our system. Besides, the density of state (DOS) and conductance are also studied.

## II. MODEL AND NOTATION

In this paper, we consider a double quantum dot system in which the QDs are coupled with the single mode detuning quantum photon field. The sketch of the system is plotted in Fig. 1. Our system can be divided into two subsystems. Each subsystem contains a quantum dot and two connected leads. The electron can transit between the QDs in the subsystems via the electron-photon interaction in which the tunneling barrier between the QDs is incorporated with the electron-photon coupling constant $M$.

The Hamiltonian can be expressed as

$$H = \sum_{m\in 1,2} H_m + H_{e\text{-}ph} + H_{ph}, \tag{1}$$

where

$$H_m = H_{QD,m} + H_{lead,m} + H_{T,m}, \tag{2}$$

$$H_{QD,m} = \varepsilon_m d_m^+ d_m + U\hat{n}_m\hat{n}_{\bar{m}}, \tag{3}$$

$$H_{lead,m} = \sum_{\substack{k_{m,\alpha}\\ \alpha\in L,R}} \epsilon_{k_{\alpha,m}} c_{k_{\alpha,m}}^+ c_{k_{\alpha,m}}, \tag{4}$$

$$H_{T,m} = \sum_{\substack{k_{m,\alpha}\\ \alpha\in L,R}} V_{m,\alpha} c_{k_{\alpha,m}}^+ d_m + \text{H.c.}, \tag{5}$$

$$H_{ph} = \omega_{ph} b^+ b, \tag{6}$$

$$H_{e\text{-}ph} = M d_2^+ b d_1 + \text{H.c.} \tag{7}$$

The Hamiltonian $H$ includes three parts. The first term in Eq. (1) is the Hamiltonian of individual subsystems. The second term in Eq. (1) is the electron-photon interaction Hamiltonian. The subsystems interact with each other and the electron transits between the subsystems via the electron-photon interaction. The third term is the energy of the photon cavity. The Hamiltonian of the $m$th subsystem contains the quantum dot energy $H_{QD,m}$, where $m\in 1,2$ labels the lower energy system (subsystem1) and higher energy system (subsystem2). $H_{lead,m}$ is the lead energy and $H_{T,m}$ is the tunneling Hamiltonian. The operators $d_m^\dagger$ $(d_m)$, $c_{k_{\alpha,m}}^\dagger$ $(c_{k_{\alpha,m}})$, and $b^\dagger(b)$ are the creation (annihilation) operators of electron in QD, the lead $\alpha$ in the $m$th subsystem, and the photon, respectively. $V_{\alpha,m}$ is the tunneling matrix element for electron tunneling between QD and lead $\alpha$ in the subsystem $m$.

In order to simplify the problem, the following assumptions are made. (1) The tunneling matrix elements $V_{\alpha,m}$ are set to be identical for each tunneling barrier and hence the tunneling coupling constant $\Gamma_{m,\alpha}=\Gamma/2$. (2) The electron-photon interaction is assumed in the dipole approximation and the corresponding Hamiltonian is $H_{e\text{-}ph}$, where $M$ is the electron-photon coupling coefficient.[24] (3) The tunneling barrier between the dots is involved in $M$. (4) The large photon number situation, i.e., $n_{ph}\gg 1$, is considered.

In this paper, the notation $\Pi_{\bar{m}m}^{(\gamma)}$ $(\gamma\in \text{adj},\text{int})$ is used to label the self-energy corresponding to the EPAUT processes. Via the equation of motion method, EPAUT self-energies are obtained as

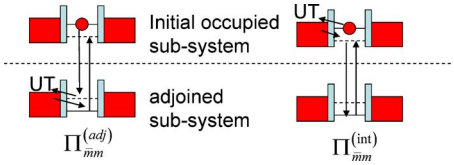


FIG. 2. (Color online) The sketch of the notation of the EPAUT coupling energy $\Pi_{m'}^{\gamma,m}$, where $\gamma\in \text{int},\text{adj}$ and $m,m'\in 1,2$.

$$\Pi_{\bar{m}m}^{(\text{adj})} = M\sum_{k_{\bar{m},\alpha}} \frac{|V_{k_{\bar{m},\alpha}}|^2}{[\omega-\varepsilon_{k_{\bar{m},\alpha}}-(-1)^m\omega_{ph}][\omega-\varepsilon_{k_{\bar{m},\alpha}}-(-1)^m(\omega_{ph}+\Delta)]} f_{k_{\bar{m},\alpha}}$$
$$= (-1)^{\bar{m}}\sum_\alpha \frac{M\Gamma_{\bar{m},\alpha}}{2\pi\Delta} \ln\frac{[\omega-\varepsilon_{\bar{m},\alpha}^F-(-1)^m(\omega_{ph}+\Delta)]^2+(\pi T)^2}{[\omega-\varepsilon_{\bar{m},\alpha}^F-(-1)^m(\omega_{ph})]^2+(\pi T)^2} \tag{8}$$

and

$$\Pi_{\bar{m}m}^{(\text{int})} = M\sum_{k_{\bar{m},\alpha}} \frac{|V_{k_{m,\alpha}}|^2}{[\omega-\varepsilon_{k_{m,\alpha}}][\omega-\varepsilon_{k_{m,\alpha}}-(-1)^m\Delta]} f_{k_{m,\alpha}}$$
$$= (-1)^{\bar{m}}\sum_\alpha \frac{M\Gamma_{m,\alpha}}{2\pi\Delta} \ln\frac{[\omega-\varepsilon_{m,\alpha}^F-(-1)^m(\Delta)]^2+(\pi T)^2}{[\omega-\varepsilon_{m,\alpha}^F)]^2+(\pi T)^2}$$
$$= (-1)^{\bar{m}}\sum_\alpha \frac{M\Gamma_{\bar{m},\alpha}}{2\pi\Delta} \ln\frac{[\omega-\varepsilon_{\bar{m},\alpha}^F-(-1)^m(\omega_{ph}+\Delta)]^2+(\pi T)^2}{[\omega-\varepsilon_{\bar{m},\alpha}^F-(-1)^m(\omega_{ph})]^2+(\pi T)^2}, \tag{9}$$

where $m,\bar{m}\in 1,2$ and $m\neq\bar{m}$. The superscript $\gamma$=adj indicates the EPAUT process that the electron in the QD of the initial occupied subsystem $m$ transits to the QD in adjoined subsystem via electron-photon interaction and then the UT proceeds between the QD and leads in the adjoined subsystem $\bar{m}$. The superscript $\gamma$=int indicates the EPAUT process that the electron proceeds the UT between QD and lead in the initial occupied subsystem $m$ and then transits to the QD in the adjointed subsystem $\bar{m}$ via the electron-photon interaction. The sketch of these two types of EPAUT is plotted in Fig. 2. It should be noted that a notation with a bar does not equal to the notation without a bar, however, a notation with a prime may equal or may not equal to the notation without a prime.

### III. CANONICAL TRANSFORMATION ANALYSIS

In order to distinguish the EPAUT from the usual Kondo effect and recognize the role of the electron-photon interaction and the tunneling processes in EPAUT, we apply the canonical transformation twice on the Hamiltonian shown in Eq. (1). The Hamiltonian Eq. (1) can be transformed into the form of the Anderson impurity model via choosing the transformation function as

$$S^{(1)} = S^{(1)}_{SW} + S^{(1)}_{e\text{-}ph}, \tag{10}$$

$$S^{(1)}_{SW} = \sum_{k_{m,\alpha}} V_{m,\alpha}\left(\frac{1-n_{\bar{m}}}{\varepsilon_m - \varepsilon_{k_m}} + \frac{n_{\bar{m}}}{\varepsilon_m + U - \varepsilon_{k_m}}\right)(d^\dagger_m c_{k_{\alpha,m}} - c^\dagger_{k_{\alpha,m}} d_m), \tag{11}$$

$$S^{(1)}_{e\text{-}ph} = \frac{M}{\Delta}(d^\dagger_2 d_1 b - b^\dagger d^\dagger_1 d_2), \tag{12}$$

keeping the terms proportional to $|M|^2$, $|V_{m,\alpha}|^2$, and $|MV_{m,\alpha}|$. The Hamiltonian in Eq. (1) is transformed as

$$\begin{aligned}\tilde{H}^{(1)} &= e^{s^{(1)}} H e^{-s^{(1)}} \simeq H_{QD} + H_{lead} + \frac{1}{2}[S^{(1)}, H_{int}] \\ &= \tilde{H}^{(1)}_0 + \tilde{H}^{(1)}_{ep\text{-}T} + H_{lead} + H_{ph},\end{aligned} \tag{13}$$

$$\tilde{H}^{(1)}_0 \equiv \tilde{H}^{(1)}_{QD} + \tilde{H}^{(1)}_K + \tilde{H}^{(1)}_{Coul}, \tag{14}$$

where

$$\tilde{H}^{(1)}_{QD} = \left[\varepsilon_1 + \frac{|M|^2}{\Delta} b^\dagger b\right] d^\dagger_1 d_1 + \left[\varepsilon_2 - \frac{|M|^2}{\Delta} b b^\dagger\right] d^\dagger_2 d_2, \tag{15}$$

$$\tilde{H}^{(1)}_{Coul} = \left[U - \frac{|M|^2}{\Delta}\right] d^\dagger_2 d_2 d^\dagger_1 d_1, \tag{16}$$

$$\begin{aligned}\tilde{H}^{(1)}_K = &\sum_{k_m, q_m} \frac{V_{k_m} V_{q_m}}{\varepsilon_m - \varepsilon_{k_m}}\left[n_m \delta_{q,k} - \frac{1}{2}(c^\dagger_{q_m} c_{km} + c^\dagger_{km} c_{q_m})\right] \\ &+ \sum_{k_m, q_m} J_{km,qm}\left[\frac{1}{2}(n_{\bar{m}} c^\dagger_{q_m} c_{km} + n_{\bar{m}} c^\dagger_{km} c_{q_m} \right. \\ &\left. + d^\dagger_m d_{\bar{m}} c^\dagger_{q_{\bar{m}}} c_{km} + d^\dagger_{\bar{m}} d_m c^\dagger_{km} c_{q_{\bar{m}}}) - n_{\bar{m}} n_m \delta_{qk}\right],\end{aligned} \tag{17}$$

$$J_{km,qm} \equiv V_{k_m} V_{q_m}\left(\frac{1}{\varepsilon_m - \varepsilon_{k_m}} - \frac{1}{\varepsilon_m + U - \varepsilon_{k_m}}\right), \tag{18}$$

where $J_{km,qm}$ is the effective exchange constant and

$$\begin{aligned}\tilde{H}^{(1)}_{ep\text{-}T} = &-\frac{1}{2}\sum_{k_1} MV_{k_1}\left(\frac{(1-n_1)}{\varepsilon_1 - \varepsilon_{k_1}} + \frac{n_1}{\varepsilon_1 + U - \varepsilon_{k_1}} - \frac{1}{\Delta}\right) \\ &\times [d^\dagger_2 c_{k1} b + b^\dagger c^\dagger_{k1} d_2] - \frac{1}{2}\sum_{k_2} MV_{k_2} \\ &\times \left(\frac{(1-n_2)}{\varepsilon_2 - \varepsilon_{k_2}} + \frac{n_2}{\varepsilon_2 + U - \varepsilon_{k_2}} + \frac{1}{\Delta}\right)[c^\dagger_{k_2} d_1 b + b^\dagger d^\dagger_1 c_{k_2}].\end{aligned} \tag{19}$$

The Hamiltonian $\tilde{H}^{(1)}_K$ is exactly the Kondo form which corresponds to the usual Kondo effect. In the Hamiltonian $\tilde{H}^{(1)}_K$, the term related to the two QD electrons which hops off the QD site to the Fermi sea and vice versa is abandoned. The Hamiltonian $\tilde{H}^{(1)}_{ep\text{-}T}$ is the electron-photon interaction associated with the tunneling processes and causes self-energy proportional to $|M|^2|V_{k_m}|^2$. The transformed Hamiltonian $\tilde{H}^{(1)}$ becomes the form of Anderson impurity model in which the tunneling term is recognized as the electron-photon interaction associated with tunneling (EPAT) process, i.e., $\tilde{H}^{(1)}_{ep\text{-}T}$, and the Coulomb interaction is modified as $U - |M|^2/\Delta$, in which $-|M|^2/\Delta$ is the electron-photon inducing effective interdot Coulomb interaction. Compared to the Kondo term $\tilde{H}^{(1)}_K$, the EPAT is the higher order process. Besides, the EPAT and Kondo terms are decoupled. Hence, the ground state of the considered system is the Kondo effect quasiparticle and is scattered by the EPAT process which will be shown in the following discussion when considered in the case of short distance.

In this paper, the highest order term we considered is only up to the term with $|M|^2 V_{k_m} V_{q_m}$ and all the other higher order terms are ignored. Since the terms result from the effective interdot Coulomb interaction, in which $-|M|^2/\Delta$ is the higher order scattering terms, i.e., the corresponding self-energy is proportional to $|M|^4$, the effective interdot Coulomb interaction is omitted. Besides, in distinguishing the EPAUT from the Kondo effect, we set the interdot Coulomb interaction as zero in the second canonical transformation. Hence, both of the Kondo term $\tilde{H}^{(1)}_K$ and the Coulomb term $\tilde{H}^{(1)}_{Coul}$ are zero and Kondo effect does not arise.

Set the Coulomb term as zero and transform the Hamiltonian Eq. (13) via the following function:

$$\begin{aligned}S^{(2)} = &\frac{1}{2}\sum_{k_{1,\alpha}} MV_{k_{1,\alpha}}\left(\frac{1}{\varepsilon_1 - \varepsilon_{k_{1,\alpha}}} + \frac{1}{\Delta}\right)\left(\frac{1}{\varepsilon_1 + \Delta}\right) \\ &\times (b^\dagger c_{k_{1,\alpha}} d_2 - d^\dagger_2 c_{k_{1,\alpha}} b) \\ &+ \frac{1}{2}\sum_{k_{2,\alpha}} MV_{k_{2,\alpha}}\left(\frac{1}{\varepsilon_2 - \varepsilon_{k_{2,\alpha}}} - \frac{1}{\Delta}\right)\left(\frac{1}{\varepsilon_2 - \Delta}\right) \\ &\times (c^\dagger_{k_{2,\alpha}} d_1 b - b^\dagger c_{k_{2,\alpha}} d_2).\end{aligned} \tag{20}$$

The Hamiltonian then becomes

$$\tilde{H}^{(2)} = \tilde{H}^{(1)}_{QD} + H_{lead} + H_{ph} + \frac{1}{2}[S^{(1)}, \tilde{H}^{(1)}_{ep\text{-}T}]$$

$$\equiv \tilde{H}^{(1)}_{QD} + \tilde{H}^{(2)}_{ep\text{-}T} + H_{lead} + H_{ph}, \quad (21)$$

where

$$\tilde{H}^{(2)}_{ep\text{-}T} = \sum_{k_{1,\alpha} q_{1,\beta}} J^{ep\text{-}T}_{1,\alpha\beta} (d_2^\dagger d_2 c^\dagger_{k_{1,\alpha}} c_{q_{1,\beta}} + c^\dagger_{k_{1,\alpha}} c_{q_{1,\beta}} b^\dagger b - \delta_{q_{1,\beta}, k_{1,\alpha}} d_2^\dagger d_2 b b^\dagger) + \sum_{k_{1,\alpha} q_{1,\beta}} J^{ep\text{-}T}_{2,\alpha\beta} (d_1^\dagger d_1 c^\dagger_{k_{2,\alpha}} c_{q_{2,\beta}} + c^\dagger_{k_{1,\alpha}} c_{q_{1,\beta}} b^\dagger b - \delta_{q_{1,\beta}, k_{1,\alpha}} d_1^\dagger d_1 b^\dagger b) \quad (22)$$

and

$$J^{ep\text{-}T}_{m,\alpha\beta} = (-1)^m \frac{|M|^2}{4} V_{k_{m,\alpha}} V_{q_{m,\beta}} \left[ \frac{1}{\varepsilon_m - \varepsilon_{k_{m,\alpha}}} - (-1)^m \frac{1}{\Delta} \right] \times \left[ \frac{1}{\varepsilon_m - \varepsilon_{q_{m,\alpha}}} - (-1)^m \frac{1}{\Delta} \right] \left[ \frac{1}{\varepsilon_m - (-1)^m \Delta} \right]. \quad (23)$$

The Hamiltonian in Eq. (22) describes the EPAUT between the QD and the lead in the adjoined subsystem with the effective coupling constant $J^{ep}_{m,\alpha\beta}$. From Eqs. (23) and (22), the coupling strength is proportional to $|M|^2 V_{k_{m,\alpha}} V_{q_{m,\beta}} \propto |M|^2 \Gamma_m$. Note that EPAUT is resulted from the electron-photon associated with tunneling process and not related to both the interdot Coulomb interaction $U$ and the effective interdot Coulomb interaction $|M|^2/\Delta$. It manifests that the EPAUT and the Kondo effect are different and not entangled. If the Coulomb interaction is considered, it is expected that the Kondo effect quasiparticle is scattered by EPAUT in which the self-energy is in the form of direct product of the Kondo quasiparticle Green's function and EPAUT coupling energy.

In following, the results are obtained via the equation of motion method (EOM) and the Lacroix's decoupling approximation is adopted.[26]

## IV. RESULTS AND DISCUSSIONS

### A. Long distance limit (the zero interdot Coulomb interaction approximation)

In order to understand the EPAUT and clarify its physical picture, we study the long distance (LD) case first. In the LD case, the interdot Coulomb interaction is ignored and the Kondo effect is not involved. The corresponding Green's function $G_{mm}$ is expressed as

$$[(g^T_{mm})^{-1} - M g^T_{\bar{m}\bar{m}} (M n_{ph} + (-1)^m \Pi^{(\mathrm{adj})}_{\bar{m}\bar{m}})] G_{mm} = 1, \quad (24)$$

which can be rewritten as

$$g^T_{\bar{m}\bar{m}} \left[ \left( \omega - \varepsilon^{eph+}_m - i\frac{\Gamma_m}{2} \right) \left( \omega - \varepsilon^{eph-}_m - i\frac{\Gamma_m}{2} \right) - (-1)^m M \Pi^{(\mathrm{adj})}_{\bar{m}\bar{m}} \right] G_{mm} = 1, \quad (25)$$

where $\varepsilon^{eph\pm}_m$ is the electron-photon cavity quasiparticle energy. The Green's functions $g^T_{mm} \equiv (\omega - \varepsilon_m + i\Gamma/2)^{-1}$ and $g^T_{\bar{m}\bar{m}} = [\omega - \varepsilon_{\bar{m}} - (-1)^m \omega_{ph}]^{-1}$ are the tunneling quasiparticle Green's functions. The energy $\Pi^{(\mathrm{adj})}_{\bar{m}\bar{m}}$ is the EPAUT coupling energy in which the UT occurs in the adjoined subsystem $\bar{m}$ ($m, \bar{m} \in 1, 2$ and $m \neq \bar{m}$). The detailed derivation of the above equations can be found in the Appendix . Since the self-energy $\Pi^{(\mathrm{adj})}_{\bar{m}\bar{m}}$ is the logarithmic function of temperature, therefore, as the Kondo temperature in Kondo effect, it is expected that there is a characteristic temperature $T_C$ corresponding to the EPAUT with the form similar to the Kondo temperature.

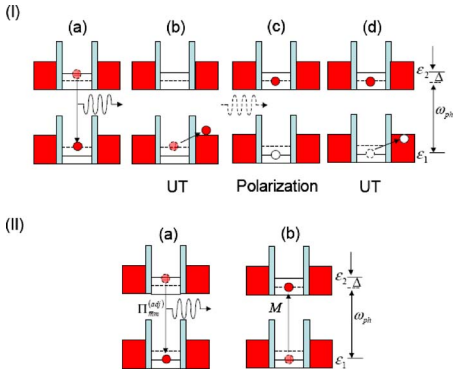


FIG. 3. (Color online) The sketch plot of the EPAUT process. (a) [process (I)] The electron in the QD2 with the resonant energy of QD2, $\omega = \varepsilon_2$, transits to QD1 with energy $\omega = \varepsilon_2 - \omega_{ph} = \varepsilon_1 + \Delta$ via emitting a photon and becomes an intermediate state. (b) The intermediate state electron tunnels out of QD1 and into lead1 via the UT. (c) The emitted photon polarizes the DQD which induces an electron in QD1 with the energy $\omega = \varepsilon_2 - \Delta$ and a hole in QD2 with the energy $\omega = \varepsilon_1$. (d) The hole tunneling into the lead 1 via UT. Process (I) can be regarded as process (II).

Equations (24) and (25) are physically meaningful. Equation (24) represents that the ground state is the tunneling quasiparticle, i.e., $g^T_{mm}$ and the ground state quasiparticle is scattered via the simple electron-photon interaction which causes the self-energy $|M|^2 n_{ph} g^T_{\bar{m}\bar{m}}$, while the EPAUT causes the self-energy $(-1)^m M g^T_{\bar{m}\bar{m}} \Pi^{(\mathrm{adj})}_{\bar{m}\bar{m}}$. Compared to the Green's function for the Kondo effect in the infinite Coulomb interaction case, Eq. (25) suggests that the tunneling related energy uncertainties are $(\varepsilon^F_m - \varepsilon^{eph+}_m)$ and $(\varepsilon^F_m - \varepsilon^{eph+}_m)$.[26]

The physical picture of the Green's function $G_{mm}$ in the LD case is demonstrated as follows. For the Green's function $G_{22}$, as shown in Fig. 3, the electron occupies the resonant state of QD2 initially with resonant energy $\varepsilon_2$, it can transit to QD1 via emitting a photon with energy $\omega_{ph}$, and it occupies the nonresonant state of QD1 with energy $\omega = \varepsilon_2 - \omega_{ph} = \varepsilon_1 + \Delta$ due to the requirement of the energy conservation. The nonresonant state electron and the emitted photon become the intermediate state. Then, there are two possible processes. The first one is the Rabi oscillation process which does not associate with the UT process and causes the self-energy $\Sigma_{Rabi} = g^T_{12} |M|^2 n_{ph}$ for the Green's function $G_{22}$. Note that there are $n_{ph}$ photons participating in the Rabi oscillation; hence, the self-energy $\Sigma_{Rabi}$ is proportional to the photon number. The second one is the electron-photon interaction associated with the uncertainty based tunneling process,

TABLE I. Comparison between the Kondo effect and EPAUT.

| | Kondo effect | EPAUT |
|---|---|---|
| Effective bandwidth | $D$ | $\lvert\Delta/\pi\rvert$ |
| Energy uncertainty | $\delta\varepsilon_0$ | $\Delta(\delta\varepsilon_m^{ph+}\delta\varepsilon_m^{ph-})$ |
| Interaction coupling strength | $\Gamma$ | $\lvert M\rvert^2\Gamma$ |

i.e., EPAUT process. The electron in QD1 with energy $\omega=\varepsilon_1+\Delta$ tunnels out of QD1 and occupies the state in lead1 with energy $\omega=\varepsilon_{k_{1\alpha}}+\Delta$. The emitted photon with energy $\omega_{ph}=\varepsilon_2-\varepsilon_1+\Delta$ causes the fluctuation of the photon cavity and thus polarizes the DQD which creates an electron with energy $\omega=\varepsilon_2-\Delta$ in QD2 and a hole with energy $\omega=\varepsilon_1$ in QD1. Finally, the hole in QD1 tunnels into lead1 and occupies the state with energy $\omega=\varepsilon_{1_{k\alpha}}$ via UT and leaves an electron in QD2 with energy $\omega=\varepsilon_2-\Delta$. Note that only the emitted photon participates in the DQD polarization process. In another viewpoint, the polarization and hole tunneling processes can be regarded as follows: an electron in lead1 with energy $\omega=\varepsilon_{1_{k\alpha}}$ tunnels into QD1 and occupies the resonant state via UT and then transits to the state of QD2 with energy $\omega=\varepsilon_2-\Delta$ via absorbing the emitted photon. The UT process provides a way for the electron transition from the nonresonant state to the resonant state. Hence, the complete EPAUT process can be regarded as follows: the electron in QD$m$ transits to the resonant state of the adjoined QD$\bar{m}$ via interacting with the detuning photon and UT. The effective coupling energy of EPAUT process is $\Pi_{\bar{m}m}^{(\mathrm{adj})}$. In the EPAUT process, the detuning factor $\Delta$ is the energy uncertainty due to the electron interacting with the detuning photon. The EPAUT must be completed within the time interval of time uncertainty $\sim 1/\lvert\Delta\rvert$; hence, the effective bandwidth corresponding to the EPAUT is expected in the same order of magnitude of $\lvert\Delta\rvert$ (or the lifetime of the intermediate state is in the same order of the magnitude of $1/\lvert\Delta\rvert$).

The characteristic temperature $T_C$ corresponding to the EPAUT can be obtained by solving the characteristic equation,

$$\mathrm{Re}[\delta\varepsilon_m^{ph+}\delta\varepsilon_m^{ph-}-(-1)^{\bar{m}}M\Pi_{\bar{m}m}^{(\mathrm{adj})}]=0, \tag{26}$$

i.e., the zero point of the real part of the denominator of the Green function, in the vicinity of the extreme values of EPAUT coupling energy $\Pi_{\bar{m}m}^{(\mathrm{adj})}$. Since the extreme values of $\Pi_{\bar{m}m}^{(\mathrm{adj})}$ are located at $\omega=\varepsilon_m^F$ and $\omega=\varepsilon_m^F-(-1)^m\Delta$, the characteristic temperature can be defined when $\varepsilon_2^F=\varepsilon_1^F+(\omega_{ph}+\Delta)$. In order to get the analytic solution, we solve the characteristic temperature in three regimes: $\lvert\Delta\rvert\gg\pi T_C$, $\lvert\Delta\rvert\sim\pi T_C$, and $\lvert\Delta\rvert\ll\pi T_C$.

(a) For the case of $\lvert\Delta\rvert\gg\pi T_C$, the characteristic temperature is calculated as

$$T_C=\left\lvert\frac{\Delta}{\pi}\right\rvert\exp\left[-\left\lvert\frac{\pi\Delta}{\lvert M\rvert^2\Gamma}\delta\varepsilon_m^{ph+}\delta\varepsilon_m^{ph-}\right\rvert\right], \tag{27}$$

which can be compared to the characteristic temperature $T_k$ of the Kondo temperature for infinite $U$ limit case,[26,33]

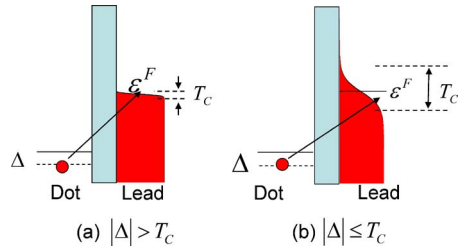


FIG. 4. (Color online) The left hand side is the dot region and the right hand side is the lead region. The red block in the right hand side is the Fermi sea. The electron transits to the dot via interacting with photon and occupies the intermediate state (dash line). The Fermi surface is smeared in higher temperature. The electron can tunnel into lead and occupied the state with energy $\omega>\varepsilon^F+T_C/2$. (a) For the case of $\lvert\Delta\rvert>T_C$, the Fermi surface is sharp and the detuning factor is important. (b) For the case of $\lvert\Delta\rvert\leqslant T_C$, the Fermi surface is smeared and the role of detuning factor is smothered.

$$T_K=D\exp\left[-\frac{\delta\varepsilon_0}{\Gamma}\right], \tag{28}$$

where $\delta\varepsilon_0\equiv(\varepsilon_F-\varepsilon_0)$. Comparing Eq. (27) with Eq. (28), the effective bandwidth, the energy uncertainties, and the interaction coupling strength for the EPAUT are able to be recognized. The comparison between the physics quantities for the Kondo effect and EPAUT are listed in Table I.

As in the preceding discussion, the EPAUT process must be completed within the time interval $1/\Delta$. Hence, $\lvert\Delta/\pi\rvert$ is the effective bandwidth in EPAUT. There are two energy uncertainties in EPAUT. One is the detuning factor $\Delta$ which is related to the electron-photon interaction and the other is $(\varepsilon_m^F-\varepsilon_m^{eph+})$ $(\varepsilon_m^F-\varepsilon_m^{eph-})$ which is related to the uncertainty based tunneling. The coupling strength in EPAUT is $\lvert M\rvert^2\Gamma$, where $M$ is related to the electron-photon interaction and $\Gamma$ is related to the uncertainty based tunneling. From Eq. (27), similar to the Kondo effect, the characteristic temperature is high when the interaction coupling constant is strong and the energy uncertainties are small.

(b) For the case of $\lvert\Delta\rvert\sim\pi T_C$, the characteristic temperature is found as

$$T_C=\frac{M\Gamma_{\bar{m}}\ln(2.618)}{2(\pi)^2\lvert(\delta\varepsilon_m^{ph+}\delta\varepsilon_m^{ph-})\rvert}. \tag{29}$$

(c) For the case of $\lvert\Delta\rvert\ll\pi T_C$, the characteristic temperature $T_C$ is obtained as

$$T_C=\frac{M\Gamma_{\bar{m}}}{2(\pi)^2(\delta\varepsilon_m^{ph+}\delta\varepsilon_m^{ph-})}. \tag{30}$$

For the $\lvert\Delta\rvert\leqslant\pi T_C$ region, the $T_C$ is independent of the detuning factor $\Delta$. As shown in Fig. 4, in the higher temperature region, the Fermi surface is smeared and the electron-photon interaction related energy uncertainty $\Delta$ is smother compared with small $T_C$. Hence, $T_C$ is dependent on the tunneling-related energy uncertainty $\delta\varepsilon_m^{ph+}\delta\varepsilon_m^{ph-}$ only. The lifetime of the corresponding quasiparticle is dominated by the UT pro-

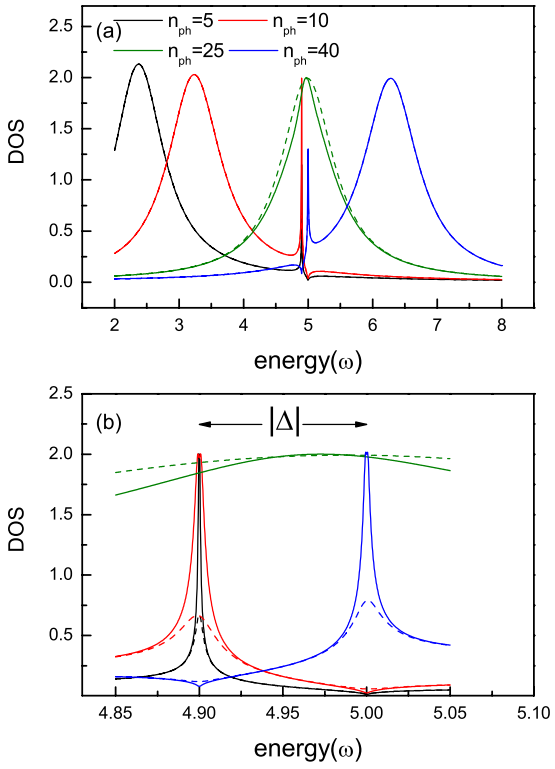


FIG. 5. (Color online) The density of state of QD2. The solid line is the case of $T=T_C$ and the dash line is the case of $T=10T_C$. The detuning factor $\Delta=0.1$. The tunneling coupling constant $\Gamma=\Gamma_m=\Gamma_m^R+\Gamma_m^L=1$. The electron-photon coupling coefficient $M=1$. The electronic energies are $\varepsilon_2^F-\varepsilon_2=\varepsilon_1^F-\varepsilon_1=5$, where $\varepsilon_1=-5$ and $\varepsilon_2=0$.

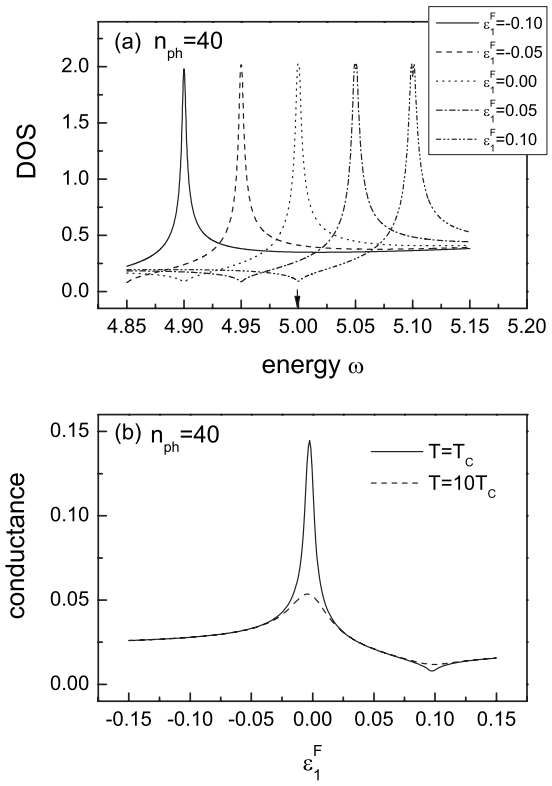


FIG. 6. (a) The DOS of QD2 and (b) the conductance of subsystem2 vs the Fermi energy of lead 1 for the case of $n_{ph}=40$. The other parameters are the same as the parameters in Fig. 5. The down arrow in (a) points the Fermi energy of lead2.

cess dominated by the uncertainty based tunneling mainly in the $|\Delta|\leqslant\pi T_C$ region.

There is a maximum solution $\pi T_C=|\Delta|$ for the case of $\varepsilon_m^F=\varepsilon_m^{eph\pm}$; i.e., the tunneling related uncertainty is zero. The maximum solution corresponds to the Rabi oscillation peak (e.g., Fig. 5, $n_{ph}=25$) and the EPAUT effect (corresponding peak) is not obvious. Besides the solution of maximum $T_C$, there is a zero $T_C$ solution for the case of large photon number, i.e., $n_{ph}\to\infty$ and $T_C\to 0$. This property reflects that the single photon fluctuation is not important and the EPAUT is weak when the photon number of the photon cavity is large in the LD case.

The densities of state of QD2 (DOS2) for the cases of $T=T_C$ and $T=10T_C$ are shown in Figs. 5(a) and 5(b). Since the poles of the self-energy $\Pi_{\bar{m}m}^{(adj)}$ are located in the vicinity of $\omega=\varepsilon_1^F+\omega_{ph}$ and are independent of the photon number $n_{ph}$, the EPAUT peaks occur in the vicinity of $\omega=\varepsilon_1^F+\omega_{ph}$ always and do not shift when the photon number $n_{ph}$ is varied. Besides, the EPAUT peak strongly depends on the temperature; hence, the EPAUT peak is weak when $T=10T_C$. The maximum value of the characteristic temperature appears in the case of $n_{ph}=25$. For the case of $n_{ph}=25$, as in the preceding discussion, the peak appeared in the vicinity of $\omega=\varepsilon_1^F+\omega_{ph}$ corresponds to the Rabi oscillation which is insensitive to the temperature.

Since the EPAUT involves two UT processes which associate with opposite charged particles, i.e., the electron and hole tunneling out of the QD1, the self-energy $\Pi_{12}^{(\mathrm{adj})}$ can be positive or negative. There are a peak and a dip in the DOS2. The peak (dip) corresponds to the electron (hole) tunneling quasiparticle. The distance of the peak and dip equals to the detuning factor $\Delta$. Besides, the sign of $\delta\varepsilon_m^{ph+}\delta\varepsilon_m^{ph-}$ changes when the Rabi oscillation peak crosses the Fermi energy $\varepsilon_2^F$; the positions of the dip and peak are exchanged for the cases of $n_{ph}<25$ and $n_{ph}>25$. For the case of $n_{ph}<25$, both the Rabi-oscillation peaks are located below the Fermi energy of the connected lead, i.e., the electron-photon interacting quasiparticle is bounded; the peak corresponding to electron UT process is below the Fermi energy. For the case of $n_{ph}>25$, the higher energy of the Rabi split peak is located at the energy higher than the Fermi energy of the connected lead, while the dip corresponding to the hole UT process is below the Fermi energy.

The conductance of subsystem2 versus the modulation of the Fermi energy of lead1, i.e., $\varepsilon_1^F$, is shown in Fig. 6. Since the electron in QD2 transits to QD1 via emitting a photon and the UT exhibits between QD1 and lead1, the EPAUT peak of DOS2 is shifted due to the modulation of the Fermi energy of lead1. Hence, the profile of the conductance becomes the mirror image of DOS2, i.e., the mirror image of Fig. 5(b). The dip of the conductance at $\varepsilon_1^F=0.1$ reflects the factor that the dip of DOS2 is pushed to $\varepsilon_2^F$ due to the raise of $\varepsilon_1^F$.

### B. Short distance limit (the infinite interdot Coulomb interaction limit)

In the short distance (SD) limit, the strong interdot Coulomb interaction is included and the electron in the adjoined QD is involved. Since the second particle (electron) is involved by the interdot Coulomb interaction, the problem becomes a two-electron system. The QD exchanges the second electron with both leads of the initial occupied and adjoining subsystems via UT processes. Besides, the backward electron may not be one of the intermediate state; hence, the exchanged electron can transit backward to initial subsystem via interacting with any one of the photon in the cavity. Therefore, there are $n_{ph}$ photons participating in the EPAUT processes and the strength of EPAUT process is enhanced with $n_{ph}$ times. Besides, as in the preceding discussion, the ground state of the QD is the Kondo effect quasiparticle when the interdot Coulomb interaction is considered.

In order to simplify the problem, the infinite interdot Coulomb interaction is considered.[23,28] Under the infinite interdot Coulomb interaction limit, the Green's functions $G_{mm}$ can be obtained as

$$[(g^K_{mm})^{-1} - n_{ph}(\mathbf{M}_{m\bar{m}})g^K_{\bar{m}m}(\mathbf{M}_{\bar{m}m})]G_{mm} = 1 - \langle n_{\bar{m}}\rangle, \quad (31)$$

where $\mathbf{M}_{\bar{m}m} \equiv M + \Pi^{(\mathrm{adj})}_{\bar{m}m} + \Pi^{(\mathrm{int})}_{\bar{m}m}$ is the generalized electron-photon coupling coefficient. The generalized electron-photon coupling coefficient involves three-electron transition processes between QDs. The first one is the simple electron-photon interaction with the coupling constant $M$. The other two are related to the EPAUT coupling energies, i.e., $\Pi^{(\mathrm{adj})}_{\bar{m}m}$ and $\Pi^{(\mathrm{int})}_{\bar{m}m}$. Equation (31) indicates that the ground state of the QD of the considered system is the Kondo effect quasiparticle and the electron-photon coupling coefficient becomes the generalized electron-photon coupling coefficient $\mathbf{M}_{\bar{m}m} \equiv M + \Pi^{(\mathrm{adj})}_{\bar{m}m} + \Pi^{(\mathrm{int})}_{\bar{m}m}$. The Kondo effect quasiparticle performs the Rabi oscillation between the DQD with the generalized electron-photon coupling coefficient $\mathbf{M}_{\bar{m}m}$.

Since the EPAUT process is involved in the generalized electron-photon coupling coefficient $\mathbf{M}_{\bar{m}m}$ and plays as a partial role in the Rabi oscillation which associates with $n_{ph}$ photons, thus the strength of the EPAUT process is enhanced by $n_{ph}$ times. It suggests that the characteristic temperature is higher than the Kondo temperature when the photon number is large enough at suitable condition. For temperature much higher than the Kondo temperature, the ground state effective quasiparticles become the tunneling quasiparticles $g^T_{mm}$ and $g^T_{\bar{m}m}$. In the following, the case beyond the Kondo effect will be discussed. We show numerically that the assumption is appropriate. Besides, since the EPAUT is enhanced by $n_{ph}$ times due to the Rabi oscillation, the DQD polarization which is induced by the single photon [the second term in square brackets of Eq. (A44)] is not important now and can be ignored.

In the SD case, $T_C$ is hardly solved in an analytic form for the finite photon number situation. In order to express the characteristic temperature in a form similar to Kondo temperature, we only take the linear terms of the EPAUT coupling energy and ignore the nonlinear terms, i.e., the product terms of $\Pi^{(\gamma)}_{m\bar{m}}$ ($\gamma \in \mathrm{adj}, \mathrm{int}$), when we solve the characteristic temperature for the finite photon situation in the SD case. Hence, the self-energy in Eq. (31) is simplified as $nMg^T_{\bar{m}m}(M + M\Pi^{(\mathrm{int})}_{\bar{m}m} + M\Pi^{(\mathrm{adj})}_{\bar{m}m} + M\Pi^{(\mathrm{int})}_{m\bar{m}} + M\Pi^{(\mathrm{adj})}_{m\bar{m}})$. Similar to the case of LD limit, we choose the condition $\varepsilon^F_{\bar{m}} + (-1)^m(\omega_{ph} + \Delta) = \varepsilon^F_m$, i.e., $\Pi^{(\mathrm{int})}_{\bar{m}m} = \Pi^{(\mathrm{adj})}_{\bar{m}m}$, to define the characteristic temperature. Hence, the characteristic equation becomes

$$\mathrm{Re}[\delta\varepsilon^{ph+}_m \delta\varepsilon^{ph-}_m - 4Mn_{ph}\Pi^{(\gamma)}_{m\bar{m}}] = 0. \quad (32)$$

Since the nonlinear terms of $\Pi^{(\gamma)}_{m\bar{m}}$ in the Green's function [Eq. (31)] are ignored in the characteristic equation, this equation does not give an exact characteristic temperature for Eq. (31). Instead of solving $T_C$ from Eq. (32) directly, we express the characteristic temperature $T_C$ by an empirical parameter $k$ multiplied by the "speculative" characteristic temperature $T^S_C$. $T^S_C$ is solved from the characteristic equation shown in Eq. (32). The characteristic temperature $T_C$ is obtained as

$$T_C = kT^S_C = k\left|\frac{\Delta}{\pi}\right| \exp\left[-\left|\frac{\pi\Delta}{4n_{ph}|M|^2\Gamma}\delta\varepsilon^{ph+}_m \delta\varepsilon^{ph-}_m\right|\right]. \quad (33)$$

The characteristic temperature shown in Eq. (33) is similar in form as that of the LD case. Figure 7 shows the characteristic temperature $T_C$ versus photon number $n_{ph}$. Similar to the case of LD limit, $T_C$ is higher when $\varepsilon^{eph\pm}_m$ is closer to the Fermi energy of the lead ($n_{ph}$=50), and $T_C$ is lower when $\varepsilon^{eph\pm}_m$ is far away from the Fermi energy of the lead. Since the EPAUT is participated by all of the photons in the cavity, the characteristic temperature for large photon number case,

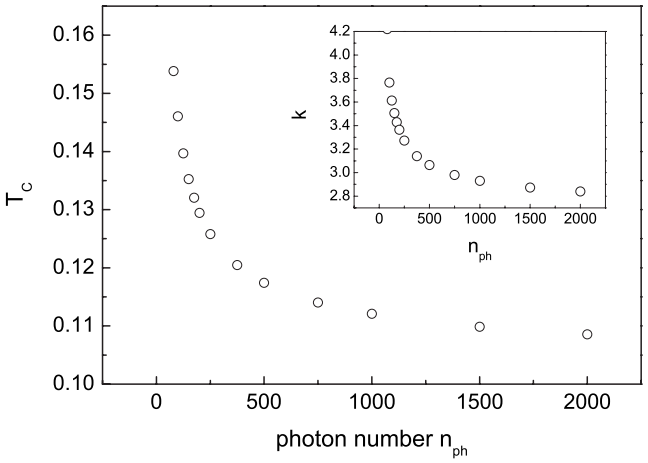


FIG. 7. The characteristic temperature versus the photon number. The related parameters are the detuning factor $\Delta$=0.1, the tunneling coupling constant $\Gamma = \Gamma_m = \Gamma^R_m + \Gamma^L_m = 1$, and the electron-photon coupling coefficient $M$=1. The electronic energy is $\varepsilon^F_2 - \varepsilon_2 = \varepsilon^F_1 - \varepsilon_1 = 5$, where $\varepsilon_1 = -5$ and $\varepsilon_2 = 0$. The corresponding Kondo temperature $T_K = 1.5 \times 10^{-5}$ for the effective bandwidth $D$=100. The inserted plot is the empirical constant $k$. The empirical constant $k$ approximates to a constant when the corresponding $T_C$ is low. It suggests that the exact form of $T_C$ for the SD case is similar to the form of $T_C$ for the LD case.

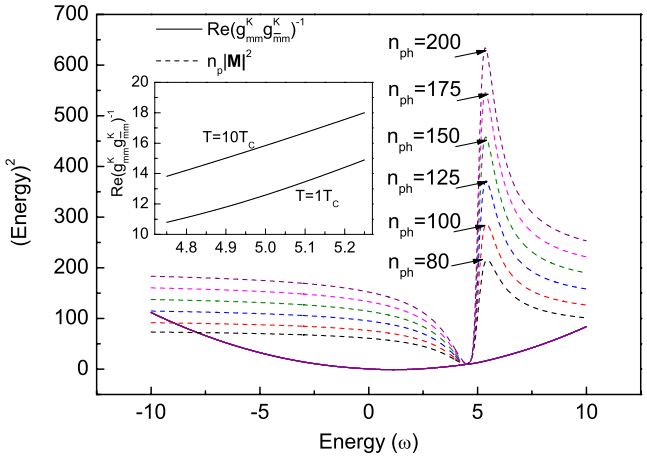


FIG. 8. (Color online) The solid lines are $\mathrm{Re}(g^K_{mm}g^K_{\bar{m}\bar{m}})^{-1}$ and the dash line are $n_{ph}|\mathbf{M}|^2 \equiv n_{ph}(\mathbf{M}_{m\bar{m}})(\mathbf{M}_{\bar{m}m})$. The inserted figures are $\mathrm{Re}(g^K_{mm}g^K_{\bar{m}\bar{m}})^{-1}$ for $n_{ph}=200$ and the temperature $T=1T_C$ and $T=10T_C$. The other related parameters are the same as Fig. 7 and $m=2$.

i.e., $n_{ph} \gg 1$, is higher than the long distance case. In the infinite photon number limit, i.e., $n_{ph} \to \infty$, the tunneling related energy uncertainty $\delta\varepsilon_m^{ph+}\delta\varepsilon_m^{ph-}$ becomes $n_{ph}|M|^2$, and the characteristic temperature, i.e., Eq. (33), is independent of the photon number $n_{ph}$. As shown in Fig. 7, the slop of the curve of the characteristic temperature versus photon number at $n_{ph}=1000$ is much smaller than the one at $n_{ph}=50$. It also implies that the characteristic temperature approximates to a constant of photon number when the photon number is infinite. Figure 8 shows $\mathrm{Re}(g^K_{mm}g^K_{\bar{m}\bar{m}})^{-1}$ and $n_{ph}|\mathbf{M}|^2 \equiv n_{ph}\mathbf{M}_{m\bar{m}}\mathbf{M}_{\bar{m}m}$. The intersection of $\mathrm{Re}(g^K_{mm}g^K_{\bar{m}\bar{m}})^{-1}$ and $n_{ph}\mathbf{M}_{m\bar{m}}\mathbf{M}_{\bar{m}m}$ shows that the obtained characteristic temperature is suitable. Besides, the inserted plot in Fig. 8 shows $\mathrm{Re}(g^K_{mm}g^K_{\bar{m}\bar{m}})^{-1}$ for the case of the temperature $T=T_C$ and $T=10T_C$. It is obvious that the change of $\mathrm{Re}(g^K_{mm}g^K_{\bar{m}\bar{m}})^{-1}$ due to the variation of temperature is much smaller than the change of $n_{ph}\mathbf{M}_{m\bar{m}}\mathbf{M}_{\bar{m}m}$. Since the Kondo effect is involved in $\mathrm{Re}(g^K_{mm}g^K_{\bar{m}\bar{m}})^{-1}$, the inserted plot in Fig. 8 points out that the Kondo effect can be ignored when $T \geqslant T_C$. It implies that the characteristic temperature of EPAUT is much higher than the Kondo temperature and agrees with our preceding argument.

In the SD case, although the characteristic temperature is hardly solved in an analytic form for the case with finite photon number, it has the analytic solution under the infinite photon number limit and is found as follows.

(a) For $|\Delta| \gg \pi T_C$,

$$T_C = \left|\frac{\Delta}{\pi}\right| \exp\left(-\left|\frac{\pi\Delta}{(2\Gamma)}\right|\right). \tag{34}$$

(b) For $|\Delta| \sim \pi T_C$,

$$T_C = \frac{2\Gamma}{2\pi^2} \ln 2.618. \tag{35}$$

(c) For $|\Delta| \ll \pi T_C$,

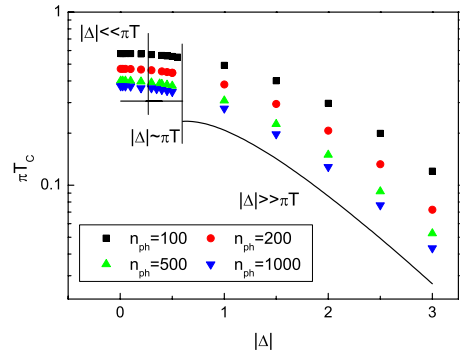


FIG. 9. (Color online) The characteristic temperature versus the detuning factor. The solid line is the case of $n_{ph} \to \infty$. The related parameters are set as $\varepsilon_2=0$, $\varepsilon_2=5$, $\varepsilon_m^F=\varepsilon_m+5$, $\Gamma_m^\alpha=\Gamma/2=0.5$, and $M=1$.

$$T_C = \frac{2\Gamma}{2\pi^2} = T_C^{\max}. \tag{36}$$

As in the preceding discussion (the finite photon case), the characteristic temperature is independent of the photon number for the case of infinite photon number. Comparing $T_C$ in the LD case, i.e., Eqs. (27), (29), and (30), and the SD case, since the UT not only proceeds in the adjoined subsystem but also in the initial occupied subsystem, therefore, the tunneling coupling strength is twice as the LD case. The plots of the characteristic temperature versus the detuning factor for various photon number cases are shown in Fig. 9. It is obvious that $T_C$ decreases exponentially as the magnitude of the detuning factor is increased in the $|\Delta| > \pi T_C$ region for any photon number. As in the preceding discussion in the LD case, the detuning factor is important and the lifetime of the corresponding quasiparticle is dominated by the detuning factor in the $|\Delta| > \pi T_C$ region. For the case of $|\Delta| \leqslant \pi T_C$, Similar to the LD case, $T_C$ is insensitive to the detuning factor and EPAUT is mainly dominated by the uncertainty based tunneling process. As shown in Eq. (36), the maximum characteristic temperature appears in the $|\Delta| \leqslant \pi T_C$ region.

Figure 10 shows the DOS of QD2 for the cases of $T=T_C$ and $T=10T_C$. The EPAUT peaks arise in the vicinity of $\omega=\varepsilon_1^F+\omega_{ph}+\Delta=\varepsilon_2^F$ when $T=T_C$ and disappear when $T=10T_C$. Compared to the LD case, the bandwidth of the EPAUT peak in the SD case is larger. This property reflects the fact of high characteristic temperature of the short distance case.

In the SD case, the EPAUT peak is due to both the UT exhibited in the initial occupied subsystem and that in the adjoined subsystem. Figure 11(a) shows the affect of EPAUT peaks of QD2 due to the modulation of the Fermi energy of lead1 and Fig. 11(b) shows the EPAUT coupling energies $\Pi_{12}^{(\mathrm{int})}$ (solid line, the UT exhibited in subsystem2) and $\Pi_{12}^{(\mathrm{adj})}$ (dash line, the UT exhibited in subsystem1) when $T=T_C$. As shown in Figs. 11(a) and 11(b), the peak height of EPAUT is shifted along the intersection of $\Pi_{12}^{(\mathrm{int})}$ and $\Pi_{12}^{(\mathrm{adj})}$ [labeled by the circle in Fig. 11(b)] when the Fermi energy of lead1 is modified. The EPAUT peak is strongest for the case of $\varepsilon_2^F=\varepsilon_1^F+(\varepsilon_2-\varepsilon_1)$ in which the $\Pi_{12}^{(\mathrm{adj})}$ and $\Pi_{12}^{(\mathrm{int})}$ overlap com-

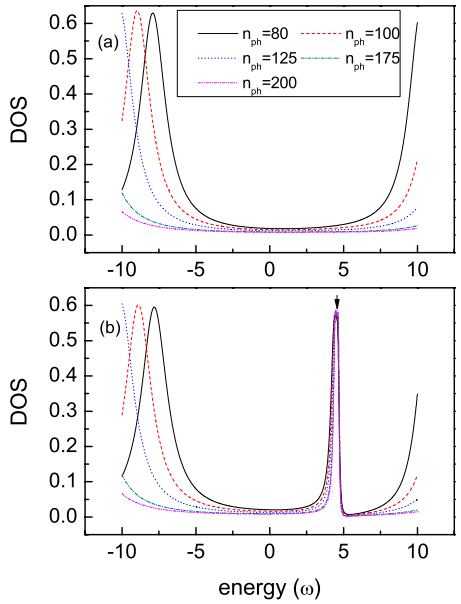


FIG. 10. (Color online) The DOS of QD2 in (a) is at $T=10T_C$ and in (b) is at $T=T_C$. The EPAUT height is pointed out by the arrow. The other related parameters are the same as Fig. 7.

pletely. When the Fermi energy of lead1, i.e., $\varepsilon_1^F$, is far away from the condition $\varepsilon_2^F=\varepsilon_1^F+(\varepsilon_2-\varepsilon_1)$, the strength of the overlap between $\Pi_{12}^{(\mathrm{adj})}$ and $\Pi_{12}^{(\mathrm{int})}$ is smaller and the EPAUT peak is weaker. Since the energy $\Pi_{12}^{(\mathrm{int})}$ is due to the UT between QD2 and lead2, it does not shift as the Fermi energy of lead1

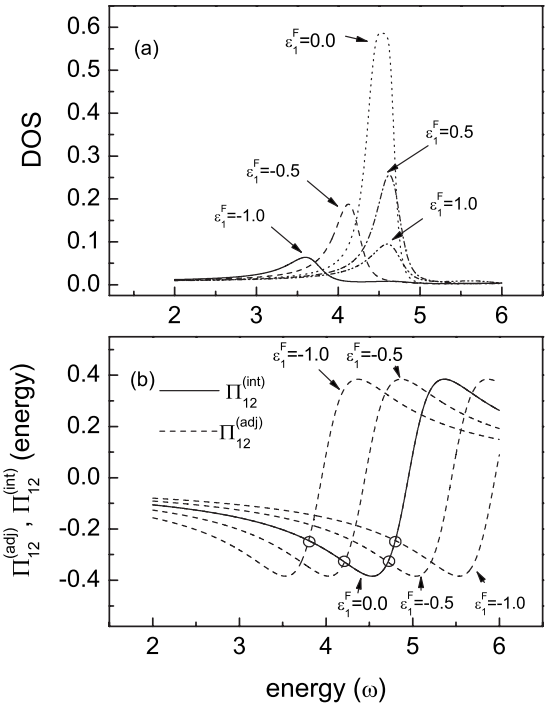


FIG. 11. (a) The DOS of QD2 for the various Fermi energy of lead2 is at $T=T_C$ ($n_{ph}=200$). (b) The EPAUT coupling energy $\Pi_{12}^{(\mathrm{int})}$ (solid line) and $\Pi_{12}^{(\mathrm{adj})}$ (dash line). The other related parameters are the same as Fig. 7.

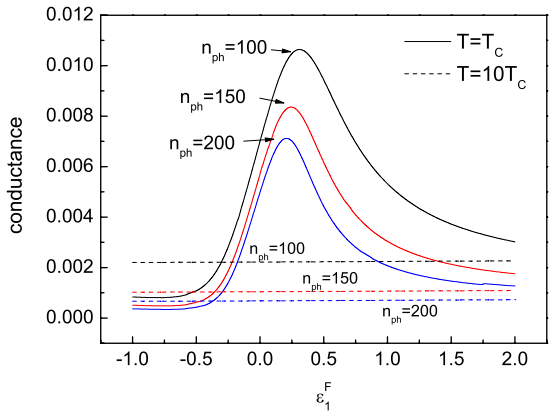


FIG. 12. (Color online) The conductance of subsystem 2 for $n_{ph}=100$, 150, and 200. The solid lines are the case of $T=T_C$ and the dash lines are the case of $T=10T_C$. The other related parameters are the same as Fig. 7.

is tuned. In the SD case, the EPAUT peak height is hardly shifted via modifying the Fermi energy of lead1. Compared to the LD case, the increase of conductance owing to tuning the Fermi energy of the lead in the adjoined subsystem is very smaller. Although the energy $\Pi_{12}^{(\mathrm{int})}$ does not shift as the variation of the Fermi energy of lead1, however, the energy $\Pi_{12}^{(\mathrm{adj})}$ is shifted. Hence, the DOS in the vicinity of $\varepsilon_2^F$ and the conductance of subsystem2 are modified slightly via tuning $\varepsilon_1^F$.

Figure 12 shows the conductance of subsystem2 versus the Fermi energy of lead1. As in the previous discussion, the conductance in the SD case is much smaller than that in the LD case. However, the increase of the conductance owing to tuning the Fermi energy of the lead in the adjoined subsystem is still prominent. The enhancement of the conductance is due to the shift of the coupling energy $\Pi_{12}^{(\mathrm{adj})}$. The conductance for the case that the EPAUT proceeds ($T=T_C$) is obviously larger than the case that the EPAUT does not proceed ($T=10T_C$). Similar to the LD case, the conductance between lead2 can be tuned by tuning the Fermi energy of lead1.

## V. CONCLUSION

We study the EPAUT in a parallel double quantum dot system. Due to the association of the UT, the electron transits between the resonant states of DQD via emitting or absorbing a detuning photon. Through the canonical analysis, EPAUT is recognized as unequal to the usual Kondo effect. For the Kondo effect, the Coulomb interaction is a necessary condition whether in the original Anderson impurity[25] model or in the extend Anderson impurity model.[28] However, unlike the usual Kondo effect, neither the interdot Coulomb interaction nor the electron-photon interaction inducing interdot Coulomb interaction is the necessary condition of EPAUT. The EPAUT results from the electron-photon interaction associated with tunneling and arises even the Coulomb interaction is zero (the LD case).

The EPAUT is studied in the LD case in which the interdot Coulomb interaction is ignored and in the SD case in

which the interdot Coulomb interaction is approximated to be infinite. In the LD case, there is only one photon participating in the EPAUT process and the uncertainty tunneling proceeds in the adjoined subsystem only. For the SD case, the UT proceeds in both the adjoined and the initial occupied subsystems and all of the photons of the photon cavity participating in the EPAUT process which becomes the partial elements of the generalized electron-photon coupling energy and plays a partial role of Rabi oscillation.

The EPAUT corresponding characteristic temperature $T_C$ is found in three regions: $|\Delta| \gg \pi T_C$, $|\Delta| \sim \pi T_C$, and $|\Delta| \ll \pi T_C$. For the $|\Delta| \gg \pi T_C$ region, $T_C$ is in the form of the Kondo temperature $T_K$. The physical quantities are recognized via comparing $T_C$ and $T_K$ and are listed in Table I. For $|\Delta| \sim \pi T_C$ and $|\Delta| \ll \pi T_C$ regions, $T_C$ is insensitive to the detuning factor and dominates by the tunneling coupling constant. For the SD case, since there are $n_{ph}$ photons participating in the EPAUT process, $T_C$ could be higher than the LD case. For suitable situation, $T_C$ is higher than the Kondo temperature in the SD case in which the interdot Coulomb interaction is involved.

The EPAUT constructs a peak of DOS of QD$m$ in the vicinity of $\omega = \varepsilon_{\bar{m}}^F + (-1)^m \omega_{ph}$ when the temperature is in the same order of magnitude of or below the characteristic temperature. The peak height of the EPAUT peak is independent of the photon number and its strength is highly sensitive to temperature; hence, it is easily differentiated from the Rabi oscillation peak.

In the LD case, UT of the EPAUT exhibits in the adjoined subsystem only. If the Fermi energy of the lead in the adjoined subsystem is tuned, the EPAUT peak will be shifted. Although the EPAUT peak is not located at the Fermi energy of connected lead always and may not contribute to the conductance, the EPAUT peak position can be shifted to the Fermi energy of the connected lead via tuning the Fermi energy of the lead in the adjoined subsystem and the electron can transport through the QD via the channel opened by the EPAUT.

In the SD case, UT is observe not only in the adjoined subsystem but also in the initial occupied subsystem and causes the EPAUT coupling energies $\Pi_{\bar{m}m}^{(\mathrm{adj})}$ and $\Pi_{\bar{m}m}^{(\mathrm{int})}$, respectively. When the lead of the subsystem is tuned toward the condition $\varepsilon_2^F = \varepsilon_1^F + (\varepsilon_2 - \varepsilon_1)$, the EPAUT coupling energies overlap completely and the EPAUT is strongest. Since the EPAUT coupling $\Pi_{\bar{m}m}^{(\mathrm{int})}$ is shifted as the Fermi energy of the connected lead is tuning and does not shift by modulating the Fermi energy of the lead in the adjoined subsystem. The EPAUT peak height is hardly to shift via modifying the Fermi energy of lead in the adjoined subsystem to open a strong channel for electron tunneling. Compared to the LD case, the conductance channel opened by the EPAUT is very weak and the conductance due to the EPAUT is very small in the SD case. However, the EPAUT still opens a weak channel for the electron transport in the SD case and the conductance is larger than the case without EPAUT ($T = 10 T_C$). Although, in the cases we considered, the EPAUT peak is located below the Fermi energy of connected lead and the conductance is small, the EPAUT peak is expected to provide the available channel for the electron transport in the nonequilibrium (finite bias) case.

The cavity QED is one of the possible mechanisms to implement the quantum information and the quantum dot is a candidate system. The semiconductor cavity QED system becomes an interested field. Most of the electron-photon interaction in the cavity QED system is independent of the electron transport. According to the EPAUT in the SD case we studied above, the electron-photon coupling coefficient is generalized as $\mathbf{M}_{\bar{m}m}$ which includes the EPAUT coupling energy. Since the EPAUT coupling energy is related to the tunneling coupling constant, the cavity QED behavior will be related to the electron transport when the QD in cavity is connected with a lead. The EPAUT provides the extra channels for the electron-photon interaction, and the strength of the electron-photon interaction can be enhanced at the suitable condition. Beside the subject of electron transport in QD system, we hope that our work will inspire the investigation on the semiconductor cavity QED systems.

## ACKNOWLEDGMENTS

This work is supported partially by the National Center for Theoretical Sciences and the National Science Council, Taiwan under Grant Nos. NSC 94-2112-M-009-024 and No. 95-2119-M-009-030.

## APPENDIX

In the following, we show the detailed derivations of the Green's functions. In the considered system, the electron transits between the QDs via the electron-photon interaction. Hence, we assume that the system is described by the diagonal Green's function $G_{mm}$ and the off-diagonal Green function $G_{m\bar{m}}$, where $m \in 1,2$ and $m \neq \bar{m}$. The main effect described in this paper contains the electron interacting with the detuning photon and the uncertainty based tunneling; hence, all of the correlation functions will be estimated in same order of magnitude of $M$ and $|V_{k_\alpha}|^2$ and expressed by the Green's functions $G_{mm}$ and $G_{m\bar{m}}$. By using the EOM method, the Green's function for QD$m$ is

$$g_{mm}^T G_{mm} = (\omega - \varepsilon_m - \Sigma^T) G_{mm} = 1 + M G_{\bar{m}m} + U G_{mm}^{(2)}, \tag{A1}$$

where $\Sigma^T = -i\Gamma/2$ is the self-energy due to the tunneling between QD and lead. In this paper, the tunneling barriers between the QD and lead are assumed identical; hence, $\Sigma_m^T = \Sigma^T = -i\Gamma/2$. The off-diagonal Green's functions are $G_{21} \equiv \langle\langle b^\dagger d_2, d_1^\dagger \rangle\rangle$ and $G_{12} \equiv \langle\langle b d_1, d_2^\dagger \rangle\rangle$. Applying the EOM on the off-diagonal Green's function, we obtain

$$\begin{aligned}(g_{\bar{m}m}^T)^{-1} G_{\bar{m}m} &\equiv (\omega - \varepsilon_m - (-1)^{\bar{m}}\Delta - \Sigma^T) G_{\bar{m}m} \\ &= (-1)^m \Pi_{\bar{m}m}^{(\mathrm{adj})} G_{mm} + M n_{ph} G_{mm} \\ &\quad + M G_{\bar{m}m}^{(dipole)} + U G_{\bar{m}m}^{(2)},\end{aligned} \tag{A2}$$

where the approximation $n_{ph} \gg 1$ is employed; hence, $\langle\langle b^\dagger b \rangle\rangle = \langle\langle b b^\dagger \rangle\rangle = n_{ph}$. The energy $\Pi_{\bar{m},m}^{(\mathrm{adj})}$ is related to the EPAUT and defined as Eq. (8).

There are two dipole-electron Green's functions which are induced by the emitted or absorbed photon,

$$G_{21}^{(dipole)} \equiv -\langle\langle d_2^\dagger d_1 d_2, d_1^\dagger\rangle\rangle, \quad G_{12}^{(dipole)} \equiv \langle\langle d_1^\dagger d_2 d_1, d_2^\dagger\rangle\rangle, \tag{A3}$$

which are induced by the electron-photon interaction. They are calculated as follows:

$$\begin{aligned}(\omega-\varepsilon_1-U)\langle\langle d_2^\dagger d_1 d_2, d_1^\dagger\rangle\rangle &= \sum_{k_{1,\alpha}} V_{k_{1,\alpha}}\langle\langle d_2^\dagger c_{k_{1,\alpha}} d_2, d_1^\dagger\rangle\rangle + \sum_{k_{2,\alpha}} V_{k_{2,\alpha}}(-\langle\langle c_{k_{2,\alpha}}^\dagger d_1 d_2, d_1^\dagger\rangle\rangle \\ &\quad + \langle\langle d_2^\dagger d_1 c_{k_{2,\alpha}}, d_1^\dagger\rangle\rangle) - MG_{21}^{(2)},\end{aligned} \tag{A4}$$

and

$$\sum_{k_{1,\alpha}} V_{k_{1,\alpha}}\langle\langle d_2^\dagger c_{k_{1,\alpha}} d_2, d_1^\dagger\rangle\rangle = \Sigma_1^T\langle\langle d_2^\dagger d_1 d_2, d_1^\dagger\rangle\rangle, \tag{A5}$$

$$\begin{aligned}\sum_{k_{2,\alpha}} -V_{k_{2,\alpha}}\langle\langle c_{k_{2,\alpha}}^\dagger d_1 d_2, d_1^\dagger\rangle\rangle &= \Sigma^{TU}\langle\langle d_2^\dagger d_1 d_2, d_1^\dagger\rangle\rangle \\ &\quad + \sum_{k_{2,\alpha}} \frac{|V_{k_{2,\alpha}}|^2}{(\omega+\varepsilon_{k_{2,\alpha}}-\varepsilon_1-\varepsilon_2-U)} f_{k_{2,\alpha}} G_{11} \\ &\equiv \Sigma^{TU}\langle\langle d_2^\dagger d_1 d_2, d_1^\dagger\rangle\rangle + K_{21,2}^{(dipole,U)} G_{11},\end{aligned} \tag{A6}$$

$$\begin{aligned}\sum_{k_{2,\alpha}} V_{k_{2,\alpha}}\langle\langle d_2^\dagger d_1 c_{k_{2,\alpha}}, d_1^\dagger\rangle\rangle &= \Sigma^T\langle\langle d_2^\dagger d_1 d_2, d_1^\dagger\rangle\rangle \\ &\quad + \sum_{k_{2,\alpha}} \frac{|V_{k_{2,\alpha}}|^2}{(\omega-\varepsilon_{k_{2,\alpha}}-\varepsilon_1+\varepsilon_2)} f_{k_{2,\alpha}} G_{11} \\ &\equiv \Sigma^T\langle\langle d_2^\dagger d_1 d_2, d_1^\dagger\rangle\rangle + K_{21,2}^{(dipole)} G_{11},\end{aligned} \tag{A7}$$

where $\Sigma^{TU} \equiv -i\Gamma/2(0)$ for finite (infinite) $U$ case. The Green's function $G_{21}^{(dipole)} \equiv -\langle\langle d_2^\dagger d_1 d_2, d_1^\dagger\rangle\rangle$ is obtained as

$$G_{21}^{(dipole)} = -g_{11}^{T(2)}(K_{21,2}^{(dipole)} + K_{21,2}^{(dipole,U)})G_{11} + g_{11}^{T(2)} M G_{21}^{(2)}, \tag{A8}$$

where $g_{11}^{T(2)} \equiv (\omega-\varepsilon_1-2\Sigma^T-\Sigma^{TU}-U)$. As the same way,

$$\begin{aligned}(\omega-\varepsilon_2-2\Sigma^T-\Sigma^{TU}-U)\langle\langle d_1^\dagger d_2 d_1, d_2^\dagger\rangle\rangle &= +\sum_{k_{2,\alpha}} V_{k_{2,\alpha}}\langle\langle d_1^\dagger c_{k_{2,\alpha}} d_1, d_2^\dagger\rangle\rangle \\ &\quad + \sum_{k_{1,\alpha}} V_{k_{1,\alpha}}(\langle\langle d_1^\dagger d_2 c_{k_{1,\alpha}}, d_2^\dagger\rangle\rangle - \langle\langle c_{k_{1,\alpha}}^\dagger d_2 d_1, d_2^\dagger\rangle\rangle) - MG_{12}^{(2)} \\ &= -MG_{12}^{(2)} + \sum_{k_{1,\alpha}} \frac{|V_{k_{1,\alpha}}|^2}{(\omega-\varepsilon_{k_{1,\alpha}}+\varepsilon_1-\varepsilon_2)} f_{k_{1,\alpha}} G_{22} \\ &\quad + \sum_{k_{1,\alpha}} \frac{|V_{k_{1,\alpha}}|^2}{(\omega+\varepsilon_{k_{1,\alpha}}-\varepsilon_1-\varepsilon_2-U)} f_{k_{1,\alpha}} G_{22} \\ &\equiv (K_{12,1}^{(ep)} + K_{12,1}^{(ep)})G_{22} - MG_{12}^{(2)}.\end{aligned} \tag{A9}$$

Hence, the Green's function $G_{12}^{(dipole)} \equiv \langle\langle d_1^\dagger d_2 d_1, d_2^\dagger\rangle\rangle$ is obtained as

$$G_{12}^{(dipole)} = g_{22}^{T(2)}(K_{12,1}^{(dipole)} + K_{12,1}^{(dipole,U)})G_{22} - g_{22}^{T(2)} M G_{12}^{(2)}. \tag{A10}$$

Hence, the off-diagonal Green's functions become

$$\begin{aligned}(g_{\bar{m}m}^T)^{-1} G_{\bar{m}m} &= [Mn_{ph} + (-1)^m \Pi_{\bar{m}m}^{(adj)} + (-1)^m M g_{mm}^{T(2)} \\ &\quad \times (K_{mm,\bar{m}}^{(dipole)} + K_{mm,\bar{m}}^{(dipole,U)})]G_{mm} \\ &\quad + (U-(-1)^m g_{mm}^{T(2)}|M|^2) G_{\bar{m}m}^{(2)}.\end{aligned} \tag{A11}$$

The two-electron Green's functions are solved as follows:

$$\begin{aligned}(\omega-\varepsilon_1-U)G_{11}^{(2)} &\equiv (\omega-\varepsilon_1-U)\langle\langle n_2 d_1, d_1^\dagger\rangle\rangle \\ &= \langle n_2\rangle + MG_{21}^{(2)} + \sum_{k_{1,\alpha}} V_{k_{1,\alpha}}\langle\langle n_2 c_{k_{1,\alpha}}, d_1^\dagger\rangle\rangle \\ &\quad + \sum_{k_{2,\alpha}} V_{k_{2,\alpha}}[\langle\langle d_2^\dagger c_{k_{2,\alpha}} d_1, d_1^\dagger\rangle\rangle \\ &\quad - \langle\langle c_{k_{2,\alpha}}^\dagger d_2 d_1, d_1^\dagger\rangle\rangle],\end{aligned} \tag{A12}$$

$$\begin{aligned}\sum_{k_{1,\alpha}} V_{k_{1,\alpha}}\langle\langle n_2 c_{k_{1,\alpha}}, d_1^\dagger\rangle\rangle &= \sum_{k_{1,\alpha}} \frac{|V_{k_{1,\alpha}}|^2}{(\omega-\varepsilon_{k_{1,\alpha}})} G_{11}^{(2)} \\ &\quad - M\sum_{k_{1,\alpha}} \frac{|V_{k_{1,\alpha}}|^2}{(\omega-\varepsilon_{k_{1,\alpha}})(\omega-\varepsilon_{k_{1,\alpha}}-\Delta)} f_{k_{1,\alpha}} G_{21} \\ &\equiv \Sigma_1^T G_{11}^{(2)} - \Pi_{12}^{(int)} G_{21},\end{aligned} \tag{A13}$$

$$\begin{aligned}\sum_{k_{2,\alpha}} V_{k_{2,\alpha}}\langle\langle d_2^\dagger c_{k_{2,\alpha}} d_1, d_1^\dagger\rangle\rangle &= \sum_{k_{2,\alpha}} \frac{|V_{k_{2,\alpha}}|^2}{(\omega-\varepsilon_{k_{2,\alpha}})} G_{11}^{(2)} - \sum_{k_{2,\alpha}} \frac{|V_{k_{2,\alpha}}|^2}{(\omega-\varepsilon_{k_{2,\alpha}})} f_{k_{2,\alpha}} G_{11} \\ &\quad - M\sum_{k_{2,\alpha}} \frac{|V_{k_{2,\alpha}}|^2}{(\omega-\varepsilon_{k_{2,\alpha}}+\omega_{ph}+\Delta)(\omega-\varepsilon_{k_{2,\alpha}}+\omega_{ph})} f_{k_{2,\alpha}} G_{21} \\ &\equiv \Sigma_2^T G_{11}^{(2)} - K_{11,2} G_{11} - \Pi_{12}^{(adj)} G_{21},\end{aligned} \tag{A14}$$

$$\begin{aligned}-\sum_{k_{2,\alpha}} V_{k_{2,\alpha}}\langle\langle c_{k_{2,\alpha}}^\dagger d_2 d_1, d_1^\dagger\rangle\rangle &= \sum_{k_{2,\alpha}} \frac{|V_{k_{2,\alpha}}|^2}{(\omega-\varepsilon_{k_{2,\alpha}})} G_{11}^{(2)} \\ &\quad - \sum_{k_{2,\alpha}} \frac{|V_{k_{2,\alpha}}|^2}{(\omega-\varepsilon_{k_{2,\alpha}}-\varepsilon_2-\varepsilon_1-U)} f_{k_{2\alpha}} G_{11} \\ &\equiv \Sigma_2^{TU} G_{11}^{(2)} - K_{11,2}^U G_{11}.\end{aligned} \tag{A15}$$

Hence, the Green's function $G_{11}^{(2)}$ is obtained as

$$(g_{11}^{T(2)})^{-1}G_{11}^{(2)} \equiv (\omega - \varepsilon_1 - U - 2\Sigma^T - \Sigma^{TU})G_{11}^{(2)} = \langle n_2\rangle - (K_{11,2} + K_{11,2}^U)G_{11} - (\Pi_{12}^{(\mathrm{int})} + \Pi_{12}^{(\mathrm{adj})})G_{21} + MG_{21}^{(2)}. \tag{A16}$$

The off-diagonal elements for two particle Green's function $G_{21}^{(2)}$ is calculated as

$$g_{21}^{T(2)}G_{21}^{(2)} \equiv (\omega - \varepsilon_2 + \omega_{ph} - U)\langle\langle b^\dagger n_1 d_2, d_1^\dagger\rangle\rangle = Mn_{ph}G_{11}^{(2)} + \sum_{k_{2,\alpha}} V_{k_{2,\alpha}}\langle\langle b^\dagger n_1 c_{k_{2,\alpha}}, d_1^\dagger\rangle\rangle + \sum_{k_{1,\alpha}} V_{k_{1,\alpha}}(-\langle\langle b^\dagger c_{k_{1,\alpha}}^\dagger d_1 d_2, d_1^\dagger\rangle\rangle + \langle\langle b^\dagger d_1^\dagger c_{k_{1,\alpha}} d_2, d_1^\dagger\rangle\rangle), \tag{A17}$$

$$\sum_{k_{2,\alpha}} V_{k_{2,\alpha}}\langle\langle b^\dagger n_1 c_{k_{2,\alpha}}, d_1^\dagger\rangle\rangle = \Sigma_2^T G_{21}^{(2)} - n_{ph}\sum_{k_{2,\alpha}} \frac{M|V_{k_{2,\alpha}}|^2}{(\omega - \varepsilon_{k_{2,\alpha}} + \omega_{ph})(\omega - \varepsilon_{k_{2,\alpha}} + \omega_{ph} + \Delta)} f_{k_{2,\alpha}} G_{11} = \Sigma_2^T G_{21}^{(2)} - n_{ph}\Pi_{21}^{(\mathrm{adj})}G_{11}, \tag{A18}$$

$$-\sum_{k_{1,\alpha}} V_{k_{1,\alpha}}\langle\langle b^\dagger c_{k_{1,\alpha}}^+ d_1 d_2, d_1^\dagger\rangle\rangle = \Sigma_1^{UT} G_{21}^{(2)} - K_{21,1}^U G_{21}, \tag{A19}$$

$$\sum_{k_{1,\alpha}} V_{k_{1,\alpha}}\langle\langle b^\dagger d_1^\dagger c_{k_{1,\alpha}} d_2, d_1^\dagger\rangle\rangle = \Sigma_1^T G_{21}^{(2)} + Mn_{ph}\Sigma_1^T G_{11}^{(2)} - K_{21,1}G_{21} - n_{ph}\sum_{k_{1,\alpha}} \frac{M|V_{k_{1,\alpha}}|^2}{(\omega - \varepsilon_{k_{1,\alpha}} - \Delta)(\omega - \varepsilon_{k_{1,\alpha}})} f_{k_{1,\alpha}} G_{11} = \Sigma_1^T G_{21}^{(2)} + Mn_{ph}\Sigma_1^T G_{11}^{(2)} - K_{21,1}G_{21} - n_{ph}\Pi_{21}^{(\mathrm{int})}G_{11}. \tag{A20}$$

Hence, $G_{21}^{(2)}$ becomes

$$(g_{21}^{T(2)})^{-1}G_{21}^{(2)} = -n_{ph}(\Pi_{21}^{(\mathrm{adj})} + \Pi_{21}^{(\mathrm{int})})G_{11} + (Mn_{ph} + Mn_{ph}\Sigma_1^T)G_{11}^{(2)} - (K_{21,1} + K_{21,1}^U)G_{21}. \tag{A21}$$

As the same way, the Green's function $G_{22}^{(2)}$ is calculated as

$$(\omega - \varepsilon_2 - U)G_{22}^{(2)} \equiv (\omega - \varepsilon_2 - U)\langle\langle n_1 d_2, d_2^\dagger\rangle\rangle = \langle n_1\rangle - MG_{12}^{(2)} + \sum_{k_{2,\alpha}} V_{k_{2,\alpha}}\langle\langle n_1 c_{k_{2,\alpha}}, d_2^\dagger\rangle\rangle + \sum_{k_{1,\alpha}} V_{k_{1,\alpha}}[\langle\langle d_1^\dagger c_{k_{1,\alpha}} d_2, d_2^\dagger\rangle\rangle - \langle\langle c_{k_{1,\alpha}}^\dagger d_1 d_2, d_2^\dagger\rangle\rangle], \tag{A22}$$

$$\sum_{k_{2,\alpha}} V_{k_{2,\alpha}}\langle\langle n_1 c_{k_{2,\alpha}}, d_2^\dagger\rangle\rangle = \sum_{k_{2,\alpha}} \frac{|V_{k_{2,\alpha}}|^2}{(\omega - \varepsilon_{k_{2,\alpha}})} G_{22}^{(2)} - M\sum_{k_{2,\alpha}} \frac{|V_{k_{2,\alpha}}|^2}{(\omega - \varepsilon_{k_{2,\alpha}})(\omega - \varepsilon_{k_{2,\alpha}} + \Delta)} f_{k_{2,\alpha}} G_{12} \equiv \Sigma_2^T G_{22}^{(2)} - \Pi_{21}^{(\mathrm{int})}G_{12}, \tag{A23}$$

$$\sum_{k_{1,\alpha}} V_{k_{1,\alpha}}\langle\langle d_1^\dagger c_{k_{1,\alpha}} d_2, d_2^\dagger\rangle\rangle = \sum_{k_{1,\alpha}} \frac{|V_{k_{1,\alpha}}|^2}{(\omega - \varepsilon_{k_{1,\alpha}})} G_{22}^{(2)} - \sum_{k_{2,\alpha}} \frac{|V_{k_{1,\alpha}}|^2}{(\omega - \varepsilon_{k_{1,\alpha}})} f_{k_{1,\alpha}} G_{22} - M\sum_{k_{1,\alpha}} \frac{|V_{k_{1,\alpha}}|^2}{(\omega - \varepsilon_{k_{1,\alpha}} - \omega_{ph} - \Delta)(\omega - \varepsilon_{k_{1,\alpha}} - \omega_{ph})} f_{k_{1,\alpha}} G_{12} \equiv \Sigma_2^T G_{11}^{(2)} - K_{22,1}G_{22} - \Pi_{21}^{(\mathrm{adj})}G_{12}, \tag{A24}$$

$$-\sum_{k_{1,\alpha}} V_{k_{1,\alpha}}\langle\langle c_{k_{1,\alpha}}^\dagger d_1 d_2, d_2^\dagger\rangle\rangle = \sum_{k_{1,\alpha}} \frac{|V_{k_{1,\alpha}}|^2}{(\omega - \varepsilon_{k_{1,\alpha}})} G_{22}^{(2)} - \sum_{k_{1,\alpha}} \frac{|V_{k_{1,\alpha}}|^2}{(\omega - \varepsilon_{k_{1,\alpha}} - \varepsilon_2 - \varepsilon_1 - U)} f_{k_{1\alpha}} G_{22} = \Sigma_1^T G_{22}^{(2)} - K_{22,1}^U G_{22}. \tag{A25}$$

Hence,

$$(g_{22}^{T(2)})^{-1}G_{22}^{(2)} \equiv (\omega - \varepsilon_2 - U - 2\Sigma^T - \Sigma^{TU})G_{22}^{(2)} = \langle n_1\rangle - MG_{12}^{(2)} - (K_{22,1} + K_{22,1}^U)G_{22} - (\Pi_{21}^{(\mathrm{adj})} + \Pi_{21}^{(\mathrm{int})})G_{12}. \tag{A26}$$

The off-diagonal two-particle Green's function $G_{12}^{(2)}$ is calculated as

$$(g_{12}^{T(2)})^{-1}G_{12}^{(2)} \equiv (\omega-\varepsilon_1-\omega_{ph}-U)\langle\langle bn_2d_1,d_2^\dagger\rangle\rangle$$
$$= Mn_{ph}G_{22}^{(2)} + \sum_{k_{1,\alpha}} V_{k_{1,\alpha}}\langle\langle bn_2c_{k_{1,\alpha}},d_2^\dagger\rangle\rangle$$
$$+ \sum_{k_{2,\alpha}} V_{k_{2,\alpha}}(-\langle\langle bc_{k_{2,\alpha}}^\dagger d_2d_1,d_2^\dagger\rangle\rangle$$
$$+ \langle\langle bd_2^\dagger c_{k_{2,\alpha}}d_1,d_2^\dagger\rangle\rangle), \quad \text{(A27)}$$

$$\sum_{k_{1,\alpha}} V_{k_{1,\alpha}}\langle\langle bn_2c_{k_{1,\alpha}},d_2^\dagger\rangle\rangle$$
$$= \Sigma_1^T G_{12}^{(2)} - Mn_{ph}\sum_{k_{1,\alpha}} \frac{|V_{k_{1,\alpha}}|^2}{(\omega-\varepsilon_{k_{1,\alpha}}-\omega_{ph})(\omega-\varepsilon_{k_{1,\alpha}}-\omega_{ph}-\Delta)}$$
$$\times f_{k_{1,\alpha}}G_{22}$$
$$= \Sigma_1^T G_{12}^{(2)} - Mn_{ph}\Pi_{12}^{(\mathrm{adj})}G_{22}, \quad \text{(A28)}$$

$$-\sum_{k_{1,\alpha}} V_{k_{2,\alpha}}\langle\langle bc_{k_{2,\alpha}}^\dagger d_2d_1,d_2^\dagger\rangle\rangle = \Sigma_2^{UT}G_{21}^{(2)} - K_{12,2}^U G_{12}, \quad \text{(A29)}$$

$$\sum_{k_{2,\alpha}} V_{k_{2,\alpha}}\langle\langle bd_2^\dagger c_{k_{2,\alpha}}d_1,d_2^\dagger\rangle\rangle$$
$$= \Sigma_2^T G_{12}^{(2)} + Mn_{ph}\Sigma_2^T G_{22}^{(2)} - K_{12,2}G_{21}$$
$$- Mn_{ph}\sum_{k_{2,\alpha}} \frac{|V_{k_{2,\alpha}}|^2}{(\omega-\varepsilon_{k_{2,\alpha}}+\Delta)(\omega-\varepsilon_{k_{2,\alpha}})} f_{k_{2,\alpha}}G_{22}$$
$$= \Sigma_2^T G_{12}^{(2)} + Mn_{ph}\Sigma_2^T G_{22}^{(2)}$$
$$- K_{12,2}G_{21} - n_{ph}\Pi_{12}^{(\mathrm{int})}G_{22}. \quad \text{(A30)}$$

Hence, the Green's function $G_{12}^{(2)}$ becomes

$$(g_{12}^{T(2)})^{-1}G_{12}^{(2)} \equiv (\omega-\varepsilon_1-\omega_{ph}-2\Sigma^T-\Sigma^{UT})G_{12}^{(2)}$$
$$= -n_{ph}(\Pi_{12}^{(\mathrm{adj})}+\Pi_{12}^{(\mathrm{int})})G_{22} - (K_{12,2}+K_{12,2}^U)G_{12}$$
$$+ (Mn_{ph}+Mn_{ph}\Sigma_2^T)G_{22}^{(2)}. \quad \text{(A31)}$$

Now, the Green's functions $G_{mm}$, $G_{\bar{m}\bar{m}}$, $G_{mm}^{(2)}$, and $G_{\bar{m}\bar{m}}^{(2)}$ are obtained as follows:

$$G_{mm} = g_{mm}^T + g_{mm}^T M G_{\bar{m}\bar{m}} + g_{mm}^T U G_{mm}^{(2)}, \quad \text{(A32)}$$

$$G_{\bar{m}\bar{m}} \equiv g_{\bar{m}\bar{m}}^T\{Mn_{ph}+(-1)^m[\Pi_{\bar{m}\bar{m}}^{(\mathrm{adj})} + Mg_{mm}^{T(2)}(K_{mm,\bar{m}}^{(dipole)}$$
$$+ K_{mm,\bar{m}}^{(dipole,U)})]\}G_{mm} + g_{\bar{m}\bar{m}}^T[U-(-1)^m g_{mm}^{T(2)}|M|^2]G_{\bar{m}\bar{m}}^{(2)}, \quad \text{(A33)}$$

$$G_{mm}^{(2)} = g_{mm}^{T(2)}\langle n_{\bar{m}}\rangle - g_{mm}^{T(2)}(K_{mm,\bar{m}}+K_{mm,\bar{m}}^U)G_{mm} - g_{mm}^{T(2)}(\Pi_{m\bar{m}}^{(\mathrm{adj})}$$
$$+ \Pi_{m\bar{m}}^{(\mathrm{int})})G_{\bar{m}m} - (-1)^m g_{mm}^{T(2)}MG_{\bar{m}m}^{(2)}, \quad \text{(A34)}$$

$$G_{\bar{m}m}^{(2)} = -g_{\bar{m}m}^{T(2)}(K_{\bar{m}m,m}+K_{\bar{m}m,m}^U)G_{\bar{m}m} - g_{\bar{m}m}^{T(2)}n_{ph}(\Pi_{\bar{m}m}^{(\mathrm{adj})}$$
$$+ \Pi_{\bar{m}m}^{(\mathrm{int})})G_{mm} + g_{\bar{m}m}^{T(2)}[Mn_{ph}+Mn_{ph}\Sigma_m^T]G_{mm}^{(2)}, \quad \text{(A35)}$$

where the terms $g_{\bar{m}m}^T M g_{mm}^{T(2)}$ $(K_{mm,\bar{m}}^{(dipole)}+K_{mm,\bar{m}}^{(dipole,U)})$ $G_{mm}$ and $g_{\bar{m}m}^T g_{mm}^{T(2)}$ $|M|^2$ $G_{\bar{m}m}^{(2)}$ in the off-diagonal Green's function $G_{\bar{m}m}$ contain the product of the tunneling quasiparticle Green's functions $g_{\bar{m}m}^T$ and $g_{mm}^{T(2)}$ and are the higher order scattering. Since we consider the lowest order scattering which is related to one tunneling quasiparticle Green's function, the terms $g_{\bar{m}m}^T M g_{mm}^{T(2)}$ $(K_{mm,\bar{m}}^{(dipole)}+K_{mm,\bar{m}}^{(dipole,U)})$ $G_{mm}$ and $g_{\bar{m}m}^T g_{mm}^{T(2)}$ $|M|^2$ $G_{\bar{m}m}^{(2)}$ which contain the product of the two tunneling quasiparticle Green's functions, i.e., $g_{\bar{m}m}^T g_{mm}^{T(2)}$, will be ignored in following discussion.

### 1. Long distance limit: The zero interdot Coulomb interaction approximation

If the distance between the quantum dots are enough long and the interdot Coulomb interaction approximates to zero, the Green's functions become

$$[(g_{mm}^T)^{-1} - Mg_{\bar{m}m}^T(Mn_{ph}+(-1)^m\Pi_{\bar{m}m}^{(\mathrm{adj})})]G_{mm} = 1. \quad \text{(A36)}$$

The Green's functions can be rewritten as

$$\left[\left(\omega-\varepsilon_m^{eph+}-i\frac{\Gamma_m}{2}\right)\left(\omega-\varepsilon_m^{eph-}-i\frac{\Gamma_m}{2}\right) - (-1)^m M\Pi_{\bar{m}m}^{(\mathrm{adj})}\right]G_{mm}$$
$$= (g_{\bar{m}m}^T)^{-1}, \quad \text{(A37)}$$

where $\varepsilon_m^{eph\pm}$ is the electron-photon interacting quasi-particle energy of QD$m$ and $\Pi_{\bar{m}m}^{(\mathrm{adj})}$ is the self-energy corresponding to the EPAUT process in which the UT processes occur in the $\bar{m}$ subsystem and the EPAUT peak heights located in the vicinity of $\varepsilon_{\bar{m}}^F+(-1)^m\omega_{ph}$.

### 2. Short distance limit: The infinite Coulomb approximation

In this case, the two electron processes are induced via the Coulomb interaction. The two-electron Green's functions are $G_{mm}^{(2)}$ and $G_{\bar{m}\bar{m}}^{(2)}$. Under the infinite $U$ limit, Eqs. (A34) and (A35) become

$$G_{mm} = g_{mm}^T + g_{mm}^T M G_{\bar{m}\bar{m}} + g_{mm}^T U G_{mm}^{(2)}, \quad \text{(A38)}$$

$$G_{\bar{m}\bar{m}} = g_{\bar{m}\bar{m}}^T[Mn_{ph}+(-1)^m\Pi_{\bar{m}m}^{(\mathrm{adj})}]G_{mm} + g_{\bar{m}\bar{m}}^T U G_{\bar{m}\bar{m}}^{(2)}, \quad \text{(A39)}$$

$$UG_{mm}^{(2)} \approx -\langle n_{\bar{m}}\rangle + K_{mm,\bar{m}}G_{mm} + [\Pi_{m\bar{m}}^{(\mathrm{int})}+\Pi_{m\bar{m}}^{(\mathrm{adj})}]G_{\bar{m}m}, \quad \text{(A40)}$$

$$UG^{(2)}_{\bar{m}m} \approx K_{\bar{m}m,m}G_{\bar{m}m} + n_{ph}(\Pi^{(\mathrm{int})}_{\bar{m}m} + \Pi^{(\mathrm{adj})}_{\bar{m}m})G_{mm}. \quad \text{(A41)}$$

Substituting Eq. (A40) in Eq. (A38) and Eq. (A41) in Eq. (A39), the Green's functions $G_{mm}$ and $G_{mm}$ can be solved. Since the interdot Coulomb interaction is strong, we expand the Green's functions with the Kondo effect interacting quasiparticle $g^K_{\bar{m}m}$,

$$(g^K_{mm})^{-1}G_{mm} \equiv [(g^T_{mm})^{-1} - K_{mm,\bar{m}}]G_{mm} = 1 - \langle n_{\bar{m}}\rangle + (M + \Pi^{(\mathrm{int})}_{m\bar{m}} + \Pi^{(\mathrm{adj})}_{m\bar{m}})G_{\bar{m}m}, \quad \text{(A42)}$$

$$(g^K_{\bar{m}m})^{-1}G_{\bar{m}m} \equiv [(g^T_{\bar{m}m})^{-1} - K_{\bar{m}m,m}]G_{\bar{m}m} = [n_{ph}(M + \Pi^{(\mathrm{int})}_{\bar{m}m} + \Pi^{(\mathrm{adj})}_{\bar{m}m}) + (-1)^m\Pi^{(\mathrm{adj})}_{\bar{m}m}]G_{mm}. \quad \text{(A43)}$$

Combining Eqs. (A42) and (A43), we get the Green's function $G_{mm}$ as

$$[(g^K_{mm})^{-1} - (-1)^m M g^K_{\bar{m}m}\Pi_{\bar{m}m} - n_{ph}(\mathbf{M}_{m\bar{m}})g^K_{\bar{m}m}(\mathbf{M}_{\bar{m}m})]G_{mm} = 1 - \langle n_{\bar{m}}\rangle, \quad \text{(A44)}$$

where $\mathbf{M}_{m\bar{m}} \equiv M + \Pi^{(\mathrm{adj})}_{m\bar{m}} + \Pi^{(\mathrm{int})}_{m\bar{m}}$. The form of Eq. (A44) is same as the Green's function for the long distance case, i.e., Eq. (A36), except the term $(\mathbf{M}_{m\bar{m}})g^K_{\bar{m}m}(\mathbf{M}_{\bar{m}m})$. For the large photon case, $(\mathbf{M}_{m\bar{m}})g^K_{\bar{m}m}(\mathbf{M}_{\bar{m}m})$ is the dominative term and the term $(-1)^m M g^K_{\bar{m}m}\Pi^{(\mathrm{adj})}_{\bar{m}m}$ can be ignored.


[1] L. Kouwenhoven and C. Marcus, Phys. World **11**(6), 35 (1988).
[2] B. G. Levi, Phys. Today **49**(5), 22 (1996).
[3] S. Fafard, K. Hinzer, and S. Raymond *et al.*, Science **274**, 1350 (1996).
[4] P. Michler, A. Kiraz, C. Becher, W. V. Schoenfeld, P. M. Petroff, Lidong Zhang, E. Hu, and A. Imamoglu, Science **290**, 2282 (2000).
[5] Z. L. Yuan, B. E. Kardynal, R. M. Stevenson, A. J. Shields, C. J. Lobo, K. Cooper, N. S. Beattie, D. A. Ritchie, and M. Pepper, Science **295**, 102 (2002).
[6] Kerry J. Vahala, Nature (London) **424**, 839 (2003).
[7] E. Peter, P. Senellart, D. Martrou, A. Lemaitre, J. Hours, J. M. Gerard, and J. Bloch, Phys. Rev. Lett. **95**, 067401 (2005).
[8] E. Peter, J. Bloch, D. Martrou, A. Lemaitre, J. Hours, G. Patriarche, A. Cavanna, J. M. Gerard, S. Laurent, I. Robert-Philip, and P. Senellart, Phys. Status Solidi B **243**, 3879 (2006).
[9] K. Hennessy, A. Badolato, M. Winger, D. Gerace, M. Atature, S. Gulde, S. Falt, E. L. Hu, and A. Imamoglu, Nature (London) **445**, 896 (2007).
[10] Andrew J. Shields, Nat. Photonics **1**, 215 (2007).
[11] Daniel Loss and David P. DiVincenzo, Phys. Rev. A **57**, 120 (1998).
[12] O. Benson, C. Santori, M. Pelton, and Y. Yamamoto, Phys. Rev. Lett. **84**, 2513 (2000).
[13] D. Fattal, K. Inoue, J. Vuckovic, C. Santori, G. S. Solomon, and Y. Yamamoto, Phys. Rev. Lett. **92**, 037903 (2004).
[14] N. Akopian *et al.*, J. Appl. Phys. **101**, 081712 (2007).
[15] David M.-T. Kuo, Phys. Rev. B **74**, 115311 (2006).
[16] B. E. Kardynal, S. S. Hees, A. J. Shields, C. Nicoll, I. Farrer, and D. A. Ritchie, Appl. Phys. Lett. **90**, 181114 (2007).
[17] G. Feve, A. Mahe, J.-M. Berroir, T. Kontos, B. Placais, D. C. Glattli, A. Cavanna, B. Etienne, and Y. Jin, Science **316**, 1169 (2007).
[18] W. G. van der Wiel, T. H. Oosterkamp, S. de Franceschi, C. J. P. M. Harmans, and L. P. Kouwenhoven, in *Strongly Correlated Fermions and Bosons in Low-Dimensional Disordered Systems*, edited by I. V. Lerner *et al.* (Kluwer Academic, Dordrecht, 2002), pp. 43–68.
[19] Ph. Brune, C. Bruder, and H. Schoeller, Phys. Rev. B **56**, 4730 (1997).
[20] O. Speer, M. E. Garcia, and K. H. Bennemann, Phys. Rev. B **62**, 2630 (2000).
[21] K. C. Lin and D. S. Chuu, Phys. Rev. B **64**, 235320 (2001).
[22] A. Zrenner, E. Beham, S. Stufler, F. Findeis, M. Bichler, and G. Abstreiter, Nature (London) **418**, 612 (2002).
[23] L. Kouwenhoven and L. I. Glazman, Phys. World **14**(1), 33 (2001).
[24] *Quantum Optics*, edited by Marlan O. Scully and M. Suhail Zubairy (Cambridge University Press, Cambridge, 1997).
[25] P. W. Anderson, Phys. Rev. **124**, 41 (1961).
[26] C. Lacroix, J. Phys. F: Met. Phys. **11**, 2389 (1981).
[27] H.-G. Luo, Z.-J. Ying, and S.-J. Wang, Phys. Rev. B **59**, 9710 (1999).
[28] U. Wilhelm, J. Schmid, J. Weis, and K. Klitzing, Physica E (Amsterdam) **9**, 625 (2001); Qing-feng Sun and Hong Guo, Phys. Rev. B **66**, 155308 (2002).
[29] M. H. Hettler and H. Schoeller, Phys. Rev. Lett. **74**, 4907 (1995).
[30] Tai-Kai Ng, Phys. Rev. Lett. **76**, 487 (1996).
[31] Avraham Schiller and Selman Hershfield, Phys. Rev. Lett. **77**, 1821 (1996).
[32] Peter Nordlander, Ned S. Wingreen, Yigal Meir, and David C. Langreth, Phys. Rev. B **61**, 2146 (2000).
[33] Since we use the equation of motion method to calculate the Green's function, we compare the EPAUT characteristic temperature with the Kondo temperature solved by the same method, i.e., Ref. 26.